جمهورية العراق
وزارة التعليم العالي والبحث العلمي
جامعة بابل
كلية الهندسة
قسم الهندسة المدنية

الخصائص الديناميكية للسقوف الخرسانية المجوفة

رسالة
مقدمة الى كلِّيةِ الهندسة / جامعِة بابل وهي جزءٍ من متطلبات الحصول على درجة الماجستير
في الهندسةِ / الهندسة المدنيةِ / انشاءات

من قبل

رسل ناظم عبد الواحد محمد

أشراف

أ. م . : عبد الرضا صالح الفتلاوي

1444 A.H **2023 A.D**

Republic of Iraq
Ministry of Higher Education
and Scientific Research
Babylon University / College of Engineering
Civil Engineering Department

Dynamic Characteristic of Reinforced Concrete Hollow-Core Slabs

A Thesis
Submitted to the College of Engineering at the University of Babylon in Partial Fulfillment of the Requirements for the Degree of Master in Engineering \civil Engineering \Structures

By

Rusul Nadhem Abdullwahed mohammed

Supervised by

Asst. Prof. Abdul Ridha Saleh Al Fatlawi

2023 A.D **1444 A.H**

بسم الله الرحمن الرحيم

(قُلْ هَلْ يَسْتَوِي الَّذِينَ يَعْلَمُونَ وَالَّذِينَ لَا يَعْلَمُونَ إِنَّمَا يَتَذَكَّرُ أُولُوا الْأَلْبَابِ)

الزمر (9)

صدق الله العلي العظيم

الخلاصة

على الرغم من أن السقوف الخرسانية المجوفة تصنع كعنصر إنشائي بارتفاع صغير مقارنة بالأبعاد الأخرى. و يمكن اعتبار وزن السقف هو العامل المهيمن لوزن المبنى بأكمله وحمله الميت في معظم الحالات للمفاهيم الهيكلية الأقدم والحديثة. و تعتبر السقوف الخرسانية المجوفة بديلاً مناسبًا لمثل هذه المشكلات المذكورة أعلاه

تناولت معظم الدراسات السابقة السقوف المجوفة تجريبياً وتحليلياً وعددياً من أجل الحصول على نظرة عامة واقعية عن أدائها. وفي الوقت نفسه ، ركزت بعض هذه الدراسات على الأداء الزلزالي وحساسية الاهتزاز للهياكل التي تحتوي على وحدات سقوف خرسانية مجوفة . لذلك ، فإن دراسة الخصائص الديناميكية لوحدات السقوف المجوفة تحت أحمال التصادم أمر مهم للغاية. تركز هذه الدراسة على الأداء الديناميكي للسقوف الخرسانية المجوفة بنوعين مختلفين من التجاويف الطولية ، ولا سيما الأشكال المربعة والدائرية. و تم إجراء هذه الدراسة من أجل فهم شامل للخصائص الديناميكية والأداء الديناميكي لنظام السقوف الخرسانية المجوفة. بمعنى آخر ، تهتم هذه الدراسة بالخصائص الديناميكية للسقوف الخرسانية المجوفة التي تتعرض لحالات مختلفة من الأحمال التصادمية

كالحمل المستطيل و الحمل المثلث والحمل المثلث المتماثل و الحمل الثابت مع الزمن ومعادلات هذه الأحمال مبرمجة في نموذجين من المواد (مرنة و مرنة-بلاستيكية)، وتكون المرنة للحمل المستطيل والمثلث و الحمل المثلث المتماثل والحمل الثابت مع الزمن

و المرنة-بلاستيكية لـ (الحمل النبضي المستطيل والحمل النبضي المثلث)

في برنامج Visual Basic

علاوة على ذلك ، تم استكشاف الاستجابة الديناميكية لنظام السقوف الخرسانية المجوفة من أجل معالجة حالات فشلها تحت تأثير حالة شديدة من أحمال التصادم .

وتشير الدراسة التحليلية لنموذج السقوف الخرسانية المجوفة الى أنه من بين الحالات المختلفة للأحمال المطبقة ؛ الحمل النبضي المستطيل هو أسوأ حالة. نظرًا لأن هذه الحالة من الحمل المطبق هي الأسوأ ، لذلك يتم اختياره ليتم دراسته من خلال تحليل العناصر المحدودة بمساعدة برنامج / ABAQUS Standard Explicit 2020

فإن التماثل بالنتائج التحليلية لبرنامج ABAQUS مع النتائج التحليلية التي تم الحصول عليها من Visual Basic أقصى فرق لا تتجاوز ٪ ٩ للحمل المستطيل النبضي و ٥% للحمل المثلث النبضي . و تشير قيمة الحد الأقصى للاختلاف في النتائج التي تم الحصول عليها إلى حقيقة الافتراضات الصحيحة التي افترضتها الحلول التحليلية التي تم إجراؤها في هذه الدراسة ..

Abstract

In spite of the concrete slabs being made as a structural element with a small height/ thickness compared to other dimensions. Slab weight can be considered the dominant factor for the entire building weight and its dead load in most cases for the oldest as well as modern structural concepts. Hollow-core slab units are considered a convenient alternative for such aforesaid issues. Most of the previous studies dealt with the hollow-core slab system experimentally, analytically as well as numerically in order to get a realistic overview of its performance. Meanwhile, some of these studies focused on the seismic performance and vibration sensitivity of the structures containing hollow-core systems as slab or even wall elements. Therefore, studying the dynamic characteristics of such hollow-core slab units under impact loads is great of interest. This research study is focused on the dynamic performance of Hollow- core slabs with two different types of geometric configurations of longitudinal voids, in particular square and circle shapes. This study has been conducted for a comprehensive understanding of the dynamic characteristics and dynamic performance of the Hollow- core slab systems. In other words, this study is concerned with the dynamic characteristics of hollow-core slabs subjected to various cases of impact load (Rectangular-pulse, triangular load pulses, symmetrical triangular pulse, constant force with finite rise time) and the equations of this loads are programmed in two models of material (elastic and elasto-plastic) for (Rectangular-pulse and triangular load pulses) and only elastic model for (symmetrical triangular pulse, constant force with finite rise time) in Visual Basic program . Moreover, the dynamic response of hollow-core slab systems was explored in order to conduct its failure- modes under the

effect of a severe case of impact loads. The analytical study of the hollow slab model is indicated that among various cases of the applied loads; the rectangular-pulse load is the worst case. Since this case of the applied load is the worst, therefore, is selected to be studied by finite-element-analysis for two models rectangle and triangle pulse load with the aid of ABAQUS Standard/Explicit 2020 software. Moreover, well matching of the analysis outcomes with analytical results obtained with maximum difference does not exceed 9% for rectangle pulse load and 5% for triangle pulse load. This value of the difference of the results obtained indicates to the fact of the correct assumptions that were assumed by the analytical solutions done in this study.

Notation	
Symbol	**Definition**
Po	Maximum applied load
t	Time
t1	Maximum time
td	Load duration
tr	Load rise time
τ	Time variable
p(t)	Applied load in any time
ωn	Frequency
$\bar{\omega}$	*N*atural frequency
m	Mass
X	Displacement or deflection
F.E.A.	Finite Element Analysis
Xd	Dynamic displacement
Xs	Static deflection
D.L.F	Dynamic load factor
K	Stiffness
μ	Ductility ratio
Xel	Elastic-limit deflection
Xmax	Maximum displacement
X°	Support motion
tel	Elastic time
Rm	Maximum resistance
I	Moment of inertia of Hollow core slab
E	Modulus of elasticity of Hollow core slab
L	Length of Hollow core slab
D	Diameter of void
W	Width
H	Thickness
N	Numbers of voids
I circle	Moment of inertia of voids
r	Radius of void
H.C.S	Hollow core slab
Max.	Maximum
c	Damping cofficient

Chapter one
Introduction

1.1 Introduction

In this chapter, the great challenges in structural design are linked to modern architectural concepts as long as could be faced by the proper selection of Appropriate structural elements, the strength of construction materials as well as the frequent use of pre-stressing. also, concrete slabs were structural elements that have been made of concrete with a small height/ thickness compared to other dimensions. Slab weight can be considered the dominant factor for the entire building weight and its dead load in most cases for the oldest as well as modern architectural concepts. From the structural point of view, reducing the weight of the entire building have been give designers numerous benefits such as the ability to withstand hazards like earthquakes. Therefore, the most alternative options were to use a hollow core slab.[1] Generally, hollow core slabs are the precast concrete element and could be cast in situ as well as which that most used around the world, especially in North America and Western Europe. Like other precast elements, hollow core slabs have some potential advantages, which include the utilization of pre-stressed concrete, repeated use of forms, optimum use of materials while minimizing its waste, higher productivity, excellent quality control, fast assembly, and reduction or absence of slab supporting for a given span.[2] Specifically, regarding the hollow core slabs, the advantages which were mentioned previously extensively related to the structural and economic efficiency of floor and roof systems which can be observed the Figure 1-1.

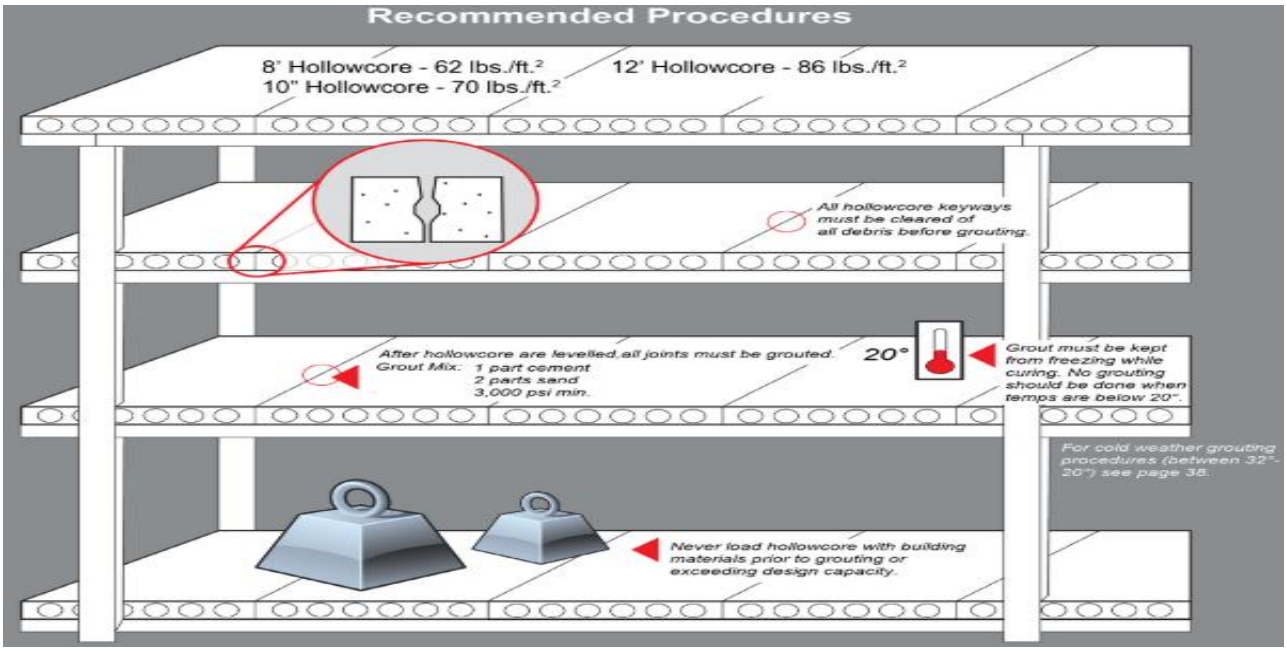

Figure 1- 1: Hollow core as the economic choice for slab system [3]

1.2 Scope of using of the hollow core slab system

Span and load characteristics, as well as requirements structural, determine the member thickness and necessary amount of pre-stressing force. As long as, most of the pioneer companies over the world in the field of production of the pre-cast concrete elements were indicated that the pre-stressed hollow core- slab was considered the appropriate choice for the slab system. This could be related to the ability of manufacturing with the longest span distance within thinner sections, lighter in weight while carrying heavier loads. There is no doubt that the capability of the indoor manufacturing as we can observed in the Plate 1-1, provide ensures consistent quality[4] allows for year-round production. Hollow-core as slab systems are providing considerable compatibility within masonry, steel, cast-in-

place, as well as other precast structures and gives design feasibility regarding to the services that could be located within cores [5].

Plate 1- 1: Indoor production line of hollow core slab [4]

Hollow core slab floors represents a specific type of slab system which made by concrete and lightened throughout its length by hollow cores. It can be with normal reinforcement or pre-stressed regarding to structural necessity. It can be noticed that the production of hollow- cores within normal reinforcement over the world wide are limited compared to the pre-stressed one. With respect for such facts, this present study will focus upon pre- stressed type only[6].

1.3 Limitations for hollow core slab system

Basically, slabs are lightened in weight by leaving longitudinal cores (voids) of acceptable size to create webs. The upper and lower flanges of these webs of the concrete section have to be pre-stressed by using embedded steel tendons. Tensioned steel is the only reinforcement in the hollow core slab, which is without reinforcement for shear resisting. Therefore, the structure's resistance to shear stresses largely depends on the tensile strength of the concrete. For this reason,

concrete quality must be controlled, constantly, as well as certified at all stages of the production line. As concerns of the shear strength capacity, which clearly depends on the concrete alone, there is an enormous mass of scientific documents on laboratory tests, in situ testing, research, studies, and codes[6]. Moreover, many reasons for inserting additional reinforcement bars into the fresh concrete of the slabs can be observed in the Figure 1-2. The designers must realize that these operations, although easily implemented, are costly and can be performed only on a limited number of slabs for a given order. [7]

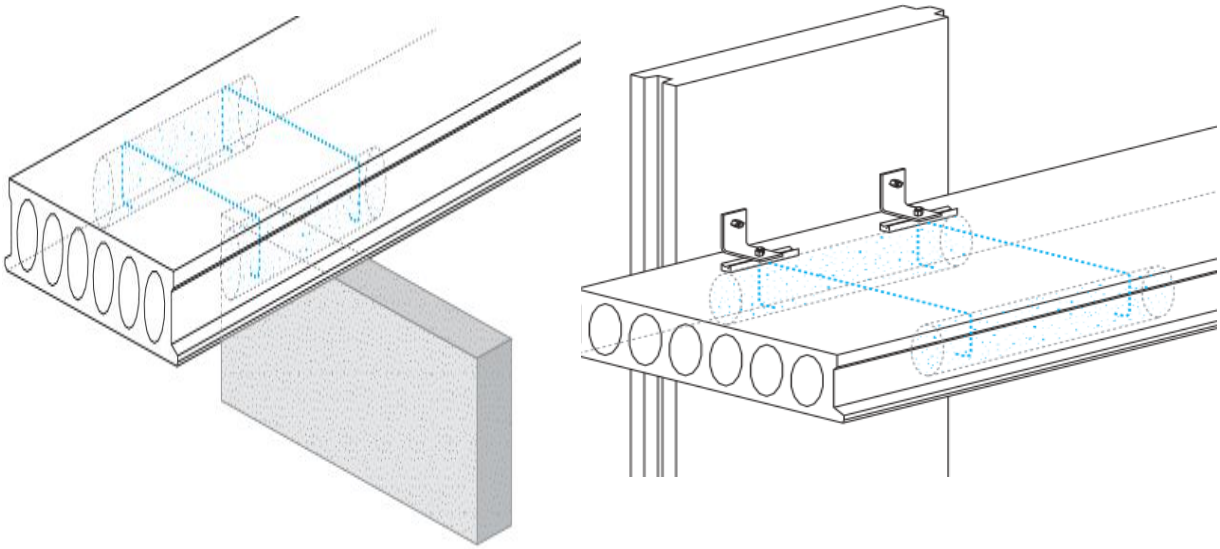

(a) (b)

Figure: 1- 2 (a) Longitudinal reinforcement inserted manually in the still-fresh concrete at support,(b) The outer edge of a hollow core slab with the proper anchoring of boltable and embedded reinforcement [8]

1.4 Applications for hollow-core slab

1.4.1 Warehouse

The buildings were constructed by steel-framed and supported on piled foundations. Precast, the pre-stressed hollow- core-panel could be easily slotted into the webs of steel columns. In the warehouse, the necessity for things was to be stored to the full height of the walls therefore, very high horizontal forces had to be taken into consideration in the design stage. The Warehouse building as shown in Plate 1-2, could consist of storage sheds within built-in galleries for ventilation and temperature control and the structures can be insulated for instance with polyurethane foam. Obviously, there is an alternative with cast concrete on-site but that would take a long time. Pre- stressed hollow- core panels would provide tolerance for normal delivery, a minimal adaptation of existing lifting gear, and very short lead-in times.[7]

Plate 1- 2: Hollow- core panels as walls in warehouse[7]

1.4.2 Flooring

Pre-stressed, hollow-core concrete slabs compared with in-situ floor casting, provide the speed of erection, lower building costs, as well as consistent quality levels which attribute with often found in one convenient package such as this kind of slab. Virtually, the slabs can be used in the construction of any type of building in which suspended floors or roofs are required. These include office blocks, flats, hostels, hospitals, factories, hotels, schools, townhouses, multi-story car parks shopping malls, and culverts.[9]

1.4.3 Security walls

There are many examples of this application for instance walls which were constructed to safeguard military equipment. The current cost of building a precast security wall shown in Plate 1-3 [10].

Plate 1- 3: Security wall that used at military zone[10]

1.4.4 Reservoirs

Hollow-core slabs are making a contribution to the storage of clean, potable water, being utilized as they are for the roofing and closure of water reservoirs. In this field of construction, it provides potential benefits which include time-saving, being the most important. and this is considered another distinct advantage indeed in the cases of fast construction necessity.[11]

1.4.5 Retaining Walls

All applications such as the retaining walls are purpose-designed to bear specific loads in particular lateral earth pressure. The time-saving factor is a major advantage here., and other advantage as the fact that construction work can continue prior to the erection of a retaining wall which usually takes place during the setting up of the floor panels. In general, a hollow-core slab is made with ready-made holes in order to facilitate lifting into the required position. [12]

1.5 The geometric configuration of the hollow section

Most of the pioneer companies in the production field of the hollow-core slab produce panels with circular sections or a hybrid circular section as shown in the Plate 1-4 below. The geometric shape of the hollow is largely related to manufacturing production lines issues structural factors. In this study, circular and square voids shapes have been utilized. from the structural point of view, there are not enough research studies regarding the geometric configuration of the void shape and its effect on the static characteristics and dynamic structural response in order to conduct possible optimizations[1-3].

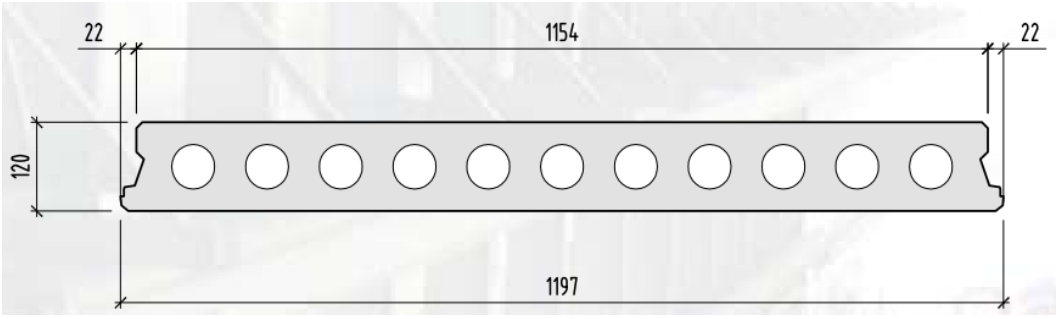

(a)

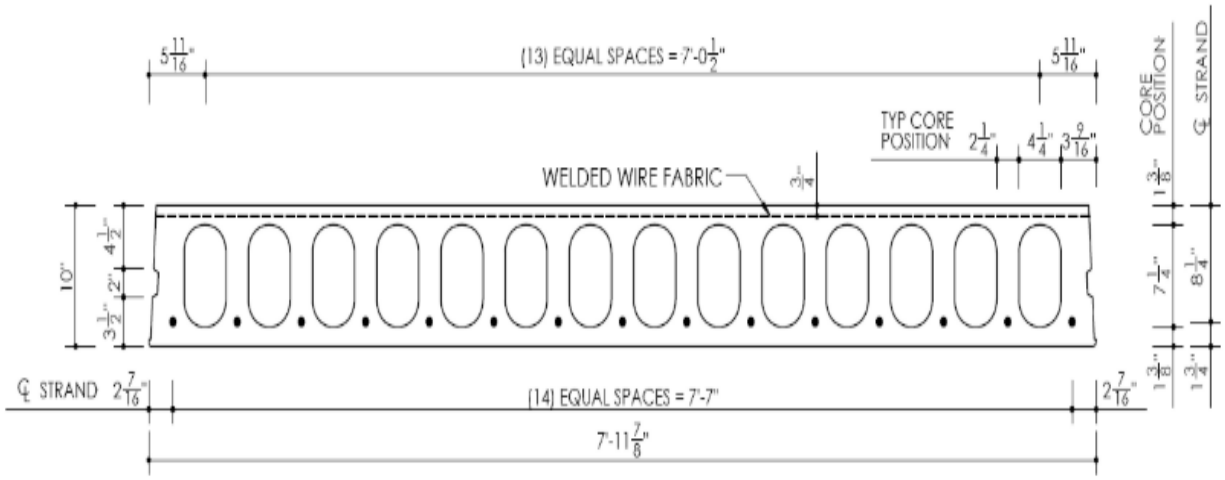

(b)

Figure 1- 3: Common geometric configurations of longitudinal voids:

(a) Circular Geometric configurations of longitudinal voids [5]

(b) Semi- circular geometric configurations of longitudinal voids[14]

1.6 Concepts of structural dynamics

From a structural engineering point of view, loads could be classified generally into static and dynamic loads. The static load is a time-independent load

that has a single response. Meanwhile, dynamic load means time-variant, in particular, the load which changes in magnitude, direction, and position and the method of action with respect to time is called dynamic loading[15]. The majority concerned for the structural engineers are accommodating that applied loads are either static or dynamic. Therefore, numerous research studies to reach a feasible understanding of structural response are subjected to various cases of loading conditions and most of these studies are about the influence of dynamic loads due to their catastrophic effect in case of the lack of consideration[16]. General classifications of dynamic loads might be as follows:

1. Periodic load

Machinery vibration (generator works within certain motor vibration). This type of the dynamic load could simple or complex harmonic loading conditions[17] as can be observed in the Figure 1-4.

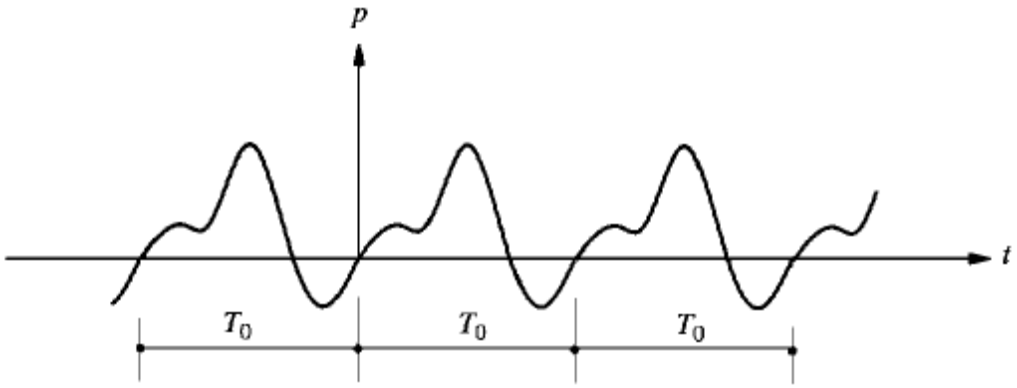

Figure 1- 4: Periodic Excitation [17]

2. Non- periodic load.

this type of non- periodic dynamic loads being either for long duration such as wind Typhoons, Cyclones, Hurricanes, and earthquake loading conditions, nor for the short duration such as blast or explosion loading conditions[17] as can be observed in the Figure 1-5.

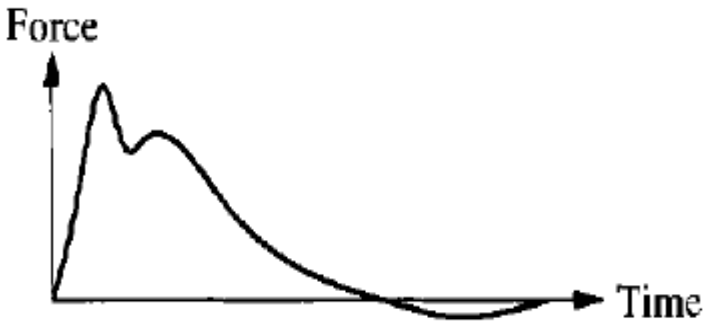

Figure 1- 5: Single pulse idealizations for air pressure generated on aboveground structure due to explosions or blast loading condition[17]

In structural dynamics point of view, other classifications are developed regarding nature of the load application with respect to time as illustrated below.

1. Prescribed loading: In this case of loading, time variation of loading is fully known, therefore deterministic analysis could be developed in order to get displacement- time history (which the focused of this study). [15]
2. Random loading: In this case of loading, time variation is not completely known but can be defined statistical sense, therefore, Non-deterministic analysis could be developed and statistical information about displacement is collected. [15]

1.7 Problem Statement

Hollow- core slab with its longitudinal voids could be potentially utilized as the economic structural elements choice for several purposes such as the applications of slab member and wall panel. This study is focused on dynamic performance of Hollow- core slab with two different type longitudinal voids, square and circle shapes. This study has been conducted for comprehensive understanding for the dynamic characteristics of impact loads represented by transient loads and dynamic performance of the Hollow- core slab.

1.8 Scope of Study

This study involves **Visual Basic Program** which are verified with the analytical solution results of **(Structural Dynamic) Handbook** and finite element analysis using **Finite Element Software ABAQUS** for Hollow- core slab under Impact loading condition (transient loads) .

This study concentrates on:

a) Dynamic characteristics of hollow- core slab subjected to impact load.

b) Dynamic response of hollow- core slab in order to conduct failure-modes under impact loads.

1.9 Thesis layout

The thesis has five chapters and it's briefed below: -

- **Chapter one:** (introduction): - This chapter adopts definition of hollow core slab, Scope of use and Application cases of hollow- core slab and most common geometric configurations of hollows. In addition to that, the chapter contains the aims of research in brief.

- **Chapter two**: (literature review): - attempt to review the past works that are related to hollow core slabs furthermore the studies in dynamic response

- **Chapter three:** - This chapter exhibits the equations and derivatives required to be programmed in the Visual Basic program and it exhibits all the analytical solutions for various cases of the applied loads (Rectangular-pulse, triangular load pulses, symmetrical triangular pulse, constant force with finite rise time) , in addition to the modelling process for carrying out finite element analysis.

- **Chapter four:** (Results and discussions): - This chapter is divided into two parts where applications are done in analysis and verification.
- **Chapter five:** (Conclusions and recommendations): - Based on the results obtained the conclusions as well as recommendations will be established.

Chapter Two
Literature Review

2.1 Introduction

This chapter describes some previous studies by other researchers that contributed the better knowledge about Hollow- core slab. Related studies on the Hollow- core slab are about its mechanical behaviour due to various loading conditions of both static as well as dynamic load. The effect of the different cases of loading is also reviewed.

2.2 Experimental Studies

Renee and Et. al. in 2004 [1], presented experimental results that were obtained to study the seismic performance of hollow-core panels utilized in the precast concrete buildings. Their experiments were established with full-scale precast concrete panels which were assemblage constructed inside the laboratory environment. Their experiments illustrate that the construction practices might be linked with poor seismic performance for pre-cast concrete hollow-core panels. Generally, the experiments were designed to investigate throughout out two-stages. Moreover, the results obtained from the second stage investigated the effectiveness of construction details practices and their seismic performance. The experiment outcomes exhibit a noticeable increase in performance for the new connection detail compared with the existing standard construction details. It exhibits relatively small amounts of damage to both, the flooring system and the frame at high lateral drift levels. The results illustrate that inter-storey drifts which excess of 3.0% can be sustained without any significant loss of support of the floor units with the improved detailing.

F. Liu., et. al in 2017 [18] presented the dynamic analysis based on experiment and numerical simulations for the hollow- core slab. In general, due to the combination of the both factors of the low self-weight and long span implies of the hollow- core slab might be caused this structural element very sensitive to vibrations that caused by human activities. Moreover, comprehensive numerical parametric analysis has been established in order to select the optimal value of the material parameters. The experiments have been performed by using a test floor consisting of 6 hollow core elements of dimension 10 m× 1.2 m× 0.27 m each and supported by steel beams. Both a vibration exciter and a force hammer have been used to load the structure. For the finite element model, solid elements have been used to model the hollow core concrete elements and the concrete joints whereas shell elements have been used to model the concrete topping as well as the supporting steel beams and columns as shown in Figure (2-1).

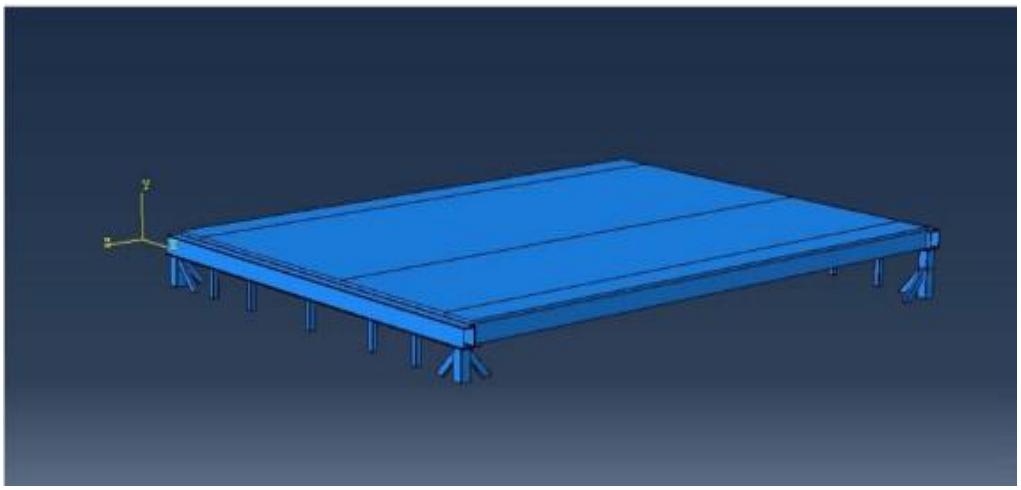

Figure 2-1: 3D finite element model [18]

Very good agreements between experimental and numerical results have been obtained especially for the two lowest modes. Parametric studies have been performed in order to determine some numerical optimal values for the elastic moduli of the concrete. The following values, expressed as a multiplicative factor of the characteristic elastic modulus have been obtained: 1.05 for the hollow core

elements, 0.55 for the joints, 0.8 for the topping. However, it must be emphasised that these factors should be considered with caution since there are based on only one experiment. The finite element model used to study the dynamic behaviour of hollow core concrete slabs with different geometries, boundary conditions and thicknesses (hollow core slabs with thickness from 200 mm to 420 mm are commonly used). As a matter of fact, by using the results obtained in the present study, it is possible to implement similar finite element models for slabs with different thicknesses and dimensions. These finite element models can be used to determine the natural frequencies of the slab and to calculate the response to harmonic

A.Maazoun, et.al in 2017 [19] investigated the deformations and failure that occur in pre-stressed and reinforced concrete hollow-core slab system in which subjected to blast loading. A four specimens of the hollow-core slabs within the compression layer and simply supported at ends were subjected to the blast loading within various standoff distances of constant charge weight of explosions as shown in Figure (2-2) .

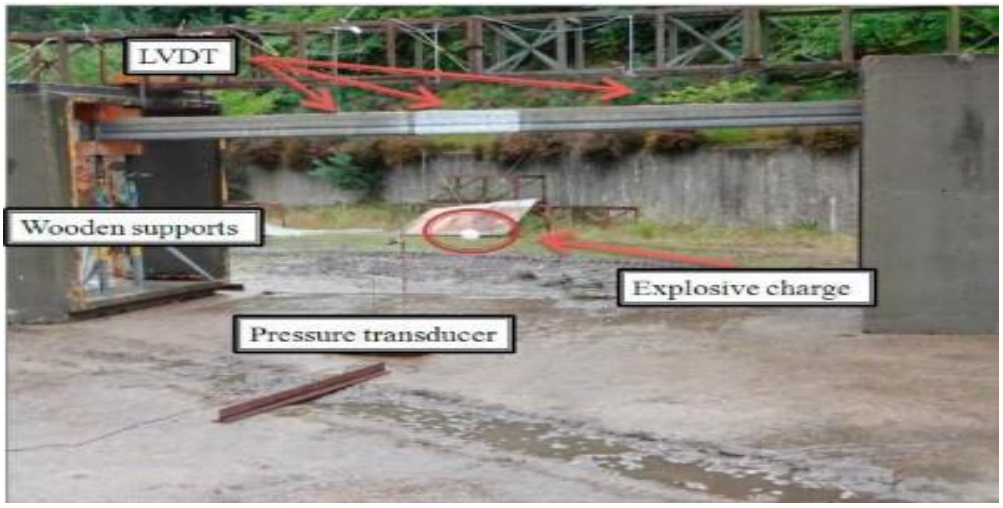

Figure 2- 2: Experimental set-up [19]

This research discusses numerical simulation outcomes, which is done by finite element software LS-DYNA explicit solver. The research study indicates that the better predications of the local and global response of the concrete element that subjected to blast loading conditions. A schematic finite element detail for RCHC with a compression layer is shown in Figure 2- 3 .

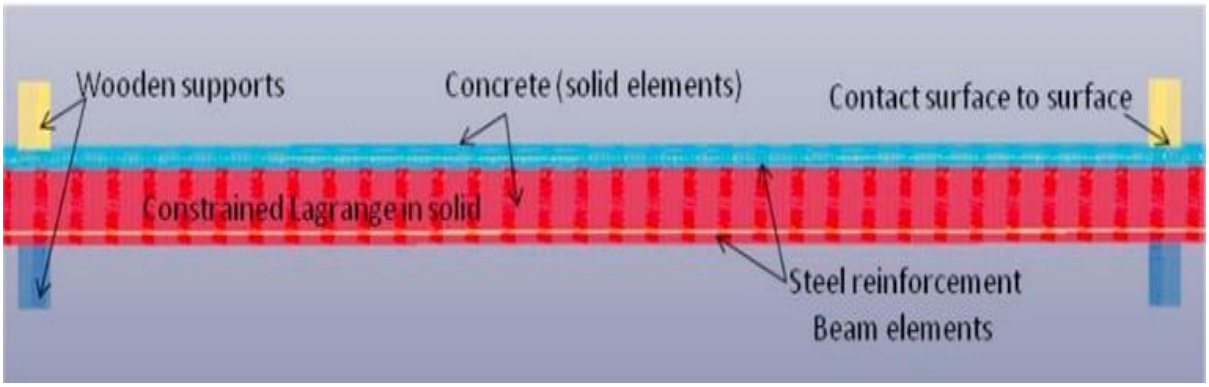

Figure 2- 3 :A schematic finite element detail for RCHC with a compression layer [19]

The outcomes of numerical analysis shows a good agreement with the experimental results for the maximum deflection at the mid span of the slabs and a good prediction of the distribution of cracks. The strain rate effect for concrete and steel are considered in this analysis. The sensitivity studies investigation the hourglass energy and the add-erosion show that these parameters have a strong effect on the dynamic response predictions of the hollow core slab under blast loading, and should be considered with care.

A. Maazoun, et.al in 2018 [20] studied the blast response within a close distance of the explosion for the retrofitted reinforced hollow-core concrete slab system . The efficiency of carbon fibre reinforced polymer CFRP, to improve blast resistance of the slab system. A studied the numerical analysis which was carried out by utilizing **LS-DYNA** software, in order to complement the experimental

results . The explosive charge of C4 was suspended from the mid-span from the underneath side of the hollow-core slab system. In terms of numerical simulation, the constant stress solid elements have been selected to represent the solid concrete part of the model. Meanwhile, Hughes-Liu beam elements have been utilized for modelling the steel reinforcement and Belytscho-Tsay shell elements for CFRP strips as the integrated elements. For the time-consuming purpose of the simulation process, a quarter of the model is considered. The shear failure surfaces which are modelled by using CDR3 includes only strain rate effect as well as damage. In another sense, the CDR3 model unable to model crack generation. Therefore, the material add- erosion must be utilized to consider the failure.

The outcomes of the study indicates significant enhancement of the resistance against the blast loading for all specimens strengthened by CFRP strips in compared with the other model. The maximum upward deflections are reduced by (16 to 30) %, meanwhile, increments have been observed on the downward deflections by (54 to 83) % when using CFRP reinforcement ratio equals $200mm^2/m$ and $250mm^2/m$, respectively. This might be related for the large part of the blast wave energy in which stored and then release to the opposite side of the slab, in particular to the main bars of steel reinforcement. The results indicate because of the propagation of the blast wave inside the concrete body, longitudinal cracks have been observed on the thin ribs between voids. Hence, the longitudinal crack will be extending into a vertical crack trigger which leading for debonding between concrete and CFRP strips. The authors indicate good agreements between experimental results and numerical outcomes.

F. Liu., et. al in 2020 [21] The finite element analysis for the dynamic response of the hollow-core panels in buildings. Was presented indicates that due to the combined influence of the low- self-weight because of the voids as well as

pre-stressing, the hollow-core panels are more sensitive to vibrations by human activities. Consequently, the necessity for modelling a finite element model is often for a better understanding of the dynamic response. This study presented six specimens in situ at four different buildings in order to perform a realistic understanding of the dynamic response of hollow-core panels. By using the finite element analysis (ABAQUS) to proposed orthotropic model for different dimensions of hollow-core panels, and studying the influence of the connections between hollow-core panels and surrounding structural elements on the dynamic behaviour of the panel. Eventually, the effect of non-bearing internal walls on the dynamic behaviour have been investigated.

This study involved obtaining the outcomes of natural frequencies and eigenvalues for different cases of the experimental tests. Clarified that both orthotropic and isotropic models have been used, in particular, four nodes doubly curved within general-purpose shell elements for modelling hollow-core panels. The steel beams, and concrete walls, were modelled by four-node shell elements. Otherwise, steel columns are modelled by two nodes with shear flexible beam elements. Convergence results are induced that the typical mesh element size is 0.05m. Tie constraints were utilized to connect the hollow-core panels to the concrete walls and to the steel beams.

Regarding experiments, very good agreements for the first, fourth, and fifth modes of natural frequencies as well as Eigen- values with finite element analysis outcomes. The concrete walls deflected within the hollow-core panels, which lead to some end moments that affect the value of the natural frequency but not notably the mode- shape. The deformations due to bending and torsional rotations have been observed within horizontal steel beams for both numerical and experimental outcomes. Three studies for not bearing internal walls are achieved. In all three

studies, accurate outcomes have been obtained, in particular for the lowest- mode. For the dynamic assessments of hollow-core panels, the lowest mode could be considered the most important one among the other modes. Regarding this fact, the not-bearing internal walls could be modelled as additional masses or even neglected. Finally, their research study concluded for the cases of dynamic assessment studies such these walls may be removed or even neglected.

Chebo, et. al, in 2022 [22] studied the structural response of hollow-core slabs subjected to low-velocity impact, which compared with the dynamic behaviour. Reinforcement concrete, and post-tensioned hollow-core slab system, have been tested under impact loading of 605 kg impactor freely dropped from specific height (14 m).The experimental modal were done for two- system of the hollow core that have been placed side by side in order to accomplish the overall width of 2400 mm.

The structural damaged occurred due to impact test cannot be strengthen or even repaired. The weakness points of the hollow core slab system have been significantly relay to the longitudinal voids, thin flanges and thin webs. Strands has no obvious influence upon resistance capacity of the load section, this might be related to the loss of continuity of webs by the fracture of one or even both flanges. The failure of hollow core slab system with topping concrete layer exhibit lower acceleration response at the edge compared with the slab center. Uncommon damping vibration have been noticed by the decaying function of the acceleration response. The indicated the reasons of this phenomena to the following reasons:

- Low acceleration amplitude after impact in added to vibration will be cause severe damage inside slab body.

- Under the impact loading condition, the hollow core slab units as representative of hollow section and the concrete topping as representative of solid section are vibrate in different manner.
- Under vertical excitation, the hollow- core slab units vibrate independently from the concrete topping because of the absence of any kind of connectors that enforcing the total thickness, eventually make it behave as the one unit.

The topping of reinforcement concrete within high compressive strength 45 MPa, enhanced hollow- core slab units for carrying additional impacts. Meanwhile, solid section of reinforced concrete still exhibits more carrying capacities in terms of cracks generation and structural failure. Filling material such as polystyrene foam can be utilized to absorb a part of the energy induced in the body of the hollow core system. In other words, the fill in material will mitigate the brittle and fracture of the thin flanges which load for enhancing the overall structural performance of the slab system.

2.3 Previous Theoretical Studies

Lara Marcos and Ricardo Carrazedo in 2014 [23] A numerical study on human-induced vibrations on hollow-core slab elements. Was presented initially, The dynamic loads have been reviewed and induced regarding the humans in activities such as walking, and acceptance criteria for human comfort were explored. A parametric study on vibration sensitivity which is done with the aid of finite element methods and numerical simulations for typical structural configurations for such structural elements. Some situations were evaluated with respect to slab thickness, different spans, and modulus of elasticity for concrete to

estimate the vibration levels. Eventually, the estimated vibration levels were compared to applicable comfort levels mentioned by international manuals and renowned authors. The results exhibit a strong increment with the peak displacements, and a small average increase with peak accelerations. However, as the thickness of the slab is increased slight reduction has been noticed with the first natural frequency, peak displacement and acceleration. On the other side, the increment of the modulus of elasticity was linked with the slight increase of the first natural frequency, displacement as well as the peak of the acceleration. They demonstrated that the estimated vibration levels might be considered adequate levels regarding the criterion of maximum dynamic displacements. Meanwhile, it could be considered inadequate according to existing limits for peak acceleration and minimum frequency. The contradiction between the occurrence of inadequate dynamic behaviour for some of the evaluated slabs emphasizes, and acceptance criteria demonstrate the importance of the continuity of this research.

M I, Rahimi, et. al in 2020 [24] investigated the ambient vibration response of hollow-core slab system by **SAP 2000** software. They focused on using finite element modelling to predict the vibration behaviour of the pre-stressed hollow-core slab system then studied vibration response through the model analysis. In general, the prediction of the floor vibration has been done by numerical analysis and the vibration performance of the actual site of floors by utilizing model analysis. The numerical analysis by using **SAP 2000** have been compared with the model analysis results obtained for the floor located in Kuala Lumpur. The multi-story office building have been constructed with concrete beams and steel I-beams, in addition to precast and pre-stressed hollow-core as slab system and in situ concrete slab for the middle- part of the office area. The finite element software SAP 2000 has been used for the modelling process in order to predict the

vibration behaviour before starting experimental works. Shell elements have been used for all parts of the floor system, with six degrees of freedom [R, R2, R3, U1, U2, and U3]. The frame elements have been used for columns and for beams.

The outcomes obtained explained that the influence of outsourced vibration, as well as noise, might lead to affect the damping ratio and cause the presence of rare mode shapes. The results exhibit frequent floor vibration might be related to a low damping ratio, and the lower the percentage of the damping ratio because of the higher of the frequency. According to the ambient test outcomes and the prediction analysis by finite element analysis results, the analysis is considered feasible due to the same range of frequency. The results of the research study demonstrated the floor is considered a low-frequency floor since the frequency obtained by the analysis is less than 10 HZ. Moreover, the low-frequency floor can be explained by several assumptions. The determinations of the vibration response by the modal testing and prediction analysis of the hollow-core slab are achieved. eventually, the results of the research indicated the weakness in the floor serviceability

2.4 Summary

In this chapter of thesis have been noticed that most previous studies involved experimental, analytical and numerical research studies. Which provides a realistic understanding of the hollow-core slab system. Some of these previous studies focused on the seismic performance of the structure containing hollow-core slab system. Other studies focused on vibration sensitivity and vibration influence on the structural behaviour for such structures containing hollow-core slab system. Meanwhile, part of the previous studies focused on the dynamic response of this type of floor while it's subjected to severe loading conditions such as blast and

impact loading conditions. Commercial finite element software packages such as **LS-DYNA, SAP 2000** as well as **ABAQUS- CAE**., might be a dominant option for numerical analysis purposes regarding reliable outcomes obtained by such software.

Chapter Three
Hollow Core Analysis

3.1 Introduction

This chapter three parts, The first part focuses the derivations of the analytical study for the four cases of load application in which Rectangular-pulse, triangular load pulses, symmetrical triangular pulse, constant force with finite rise time . The last two cases (symmetrical triangular pulse, constant force with finite rise time) of the aforesaid loading applications are derived regarding elastic range only.

Two different type of material models are considered in analysis which are elastic and elasto-plastic material models. The aforesaid material models are analysed in order to formulate derive the exact equations that describe the response of hollow-core slab regarding each case of the applied load. The second part involves utilising these derivative equations to investigate the dynamic response of the hollow-core slab units by using **Visual Basic** programming language.
meanwhile, **ABAQUS Standard/Explicit 2020** has been utilised in third part of this chapter, to investigate more realistic overview for the dynamic response of one model of the hollow-core slab.

3.2 Analytical study for various loading conditions

Analysis of any structure element involves wide investigations from the viewpoint of its strength, stiffness, stability, and vibration. Therefore, analytical studies for any structural member give the designers excellent awareness about the performance of that structural member under the applied load. From a structural point of view, to confirm any structural design must have to study the expected

applied loads, which are produced an internal forces and moments affecting the structural member. Hence, conducting an analytical study provide well knowledge about the member limitations of resisting load without showing any defects for such given applied loads.

3.2.1 Elastic Material Model

Regarding the basis of the engineering knowledge, studying the elastic stage only gives a prime overview of the mechanical properties of any materials such as bulk modulus, elastic modulus, shear modulus, Poisson ratio, etc. which are considered important parameters for the designers Analysts. Meanwhile, the material undergoes little or no yielding before rapture such as concrete, the stress-strain curve obviously exhibits that the strain value for the compression is greater than tension. Therefore, studying the elastic stage for the given structural element exhibits only a general overview of its defects.

- **Rectangular Pulse Load**

Consider the first case of a suddenly applied constant load with a limited duration td as shown in Figure 3-1 . The system starts at rest, and there is no damping .

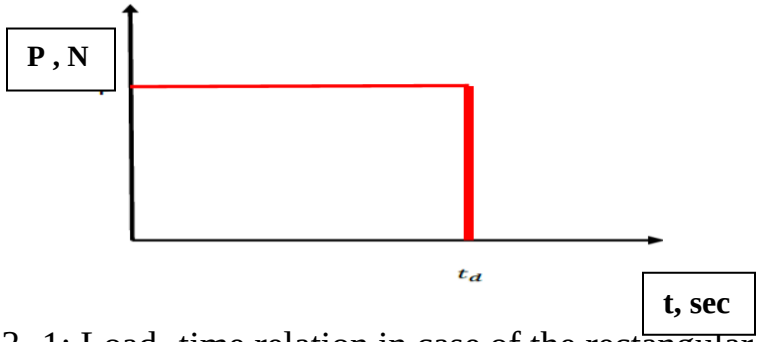

Figure 3- 1: Load- time relation in case of the rectangular pulse loading conditions

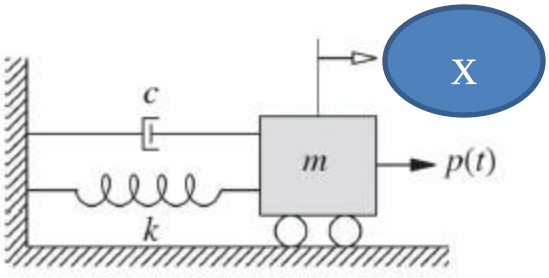

Figure 3- 2: One-dgree damped system .

Equation of motion :

$$m\ddot{x} + c\,\dot{x} + kx = 0 \qquad \text{.....(3-1)}$$

With initial conditions $\dot{x}(t) = 1/m$ and x(t) = 0

$$p(t) = p_o \qquad 0 \le t \le t_1$$

$$x = \int_0^t e^{-\gamma\,\omega_n(t-\tau)} * \sin[\bar{\omega}(t-\tau)]\,\frac{p(\tau)\,d\tau}{m\,\bar{\omega}} \qquad \text{.....(3-2)}$$

but for the c=0 the $\bar{\omega} = \omega_n \; and \; \gamma = \frac{c}{c_c} = 0$

$$\therefore x = \int_0^t \frac{p_\circ\; d\tau}{m\;\omega_n} \sin[\omega_n\,(t-\tau)] = \int_0^t \frac{p_\circ\; d\tau}{m\;\omega_n} \sin[\omega_n\,(t) - \omega_n(\tau)] * \frac{-\omega_n}{-\omega_n}$$

$$x = \frac{p_\circ}{m\,\omega_n^2}\,[\cos[\omega_n\,(t-\tau)]]_0^t \qquad \text{....(3-3)}$$

$$x_{d_t} = \frac{p_\circ}{m\,\omega_n^2}\,(1 - \cos\omega_n t)\;, 0 \le t \le t_1 \qquad \text{.....(3-4)}$$

For the free vibration loading case :

$$x = A_1 \sin[\omega_n(t - t_1)] + A_2 \cos[\omega_n(t - t_1)] \quad \ldots\ldots(3\text{-}5)$$

$$x^{\circ} = A_1\, \omega_n \cos[\omega_n\,(t - t_1)] - A_2\, \omega_n \sin[\omega_2\,(t - t_1)] \quad \ldots\ldots(3\text{-}6)$$

Similarly for the transient loading case:

$$x = \frac{p_{\circ}}{m\,\omega_n^2}\,(1 - \cos\omega_{n\,t}) \quad \ldots\ldots(3\text{-}7)$$

$$and\ x^{\circ} = \frac{p_{\circ}\ \sin\omega_n\,t}{m\,\omega_n} \quad \ldots\ldots(3\text{-}8)$$

The boundary conditions of $t = t_d$ can be used for the both cases of loading which are free vibration transient loading case.

As such, for the free vibration when $t = t_d$

$$x = A_1 \sin[\omega_n(t - t_1)] + A_2 \cos[\omega_n(t - t_1)]\ x = \frac{p_{\circ}}{m\,\omega_n^2}\,(1 - \cos\omega_{n\,t})$$

$$\frac{p_{\circ}}{m\,\omega_n^2}\,(1 - \cos\omega_{n\,t}) = A_1 \sin(0) + A_2 \cos(0)\ \ A_2 = \frac{p}{m\,\omega_n^2}\,(1 - \cos\omega_{n\,t})$$

$$at\ (t = t_1)$$

From $x^{\circ} = \frac{p_{\circ}\ \sin\omega_n\,t}{m\,\omega_n}$

$$A_1 = \frac{p_{\circ}\ \sin\omega_n\,t_1}{m\,\omega_n^2} \quad \ldots\ldots\ldots\ldots(3\text{-}9)$$

$$x_d = \frac{p_{\circ}}{m\,\omega_n^2}\,[(\sin\omega_n\,t_1) * (\sin\omega_n(t - t_1))] + \big[[1 - \cos(\omega_n\,t_1)] * [\cos(\omega_n(t - t_1))]\big] \quad \ldots\ldots\ldots\ldots(3\text{-}10)$$

For the free vibration loading case

$$x_d = \frac{p_\circ}{K}\left[\cos\left(\omega_n\,(t-t_1)\right) - \cos(\omega_n\,t)\right] \qquad \text{……(3-11)}$$

and $t = t_d$

$$D.L.F = \frac{x_d}{x_s} \qquad \text{…….(3-12)}$$

- **Triangular Pulse Load**

  Consider next a system initially at rest and subjected to a force P which has an initial , suddenly applied value of p1 and decreases linearly to zero at time td Figure 3- 3 .

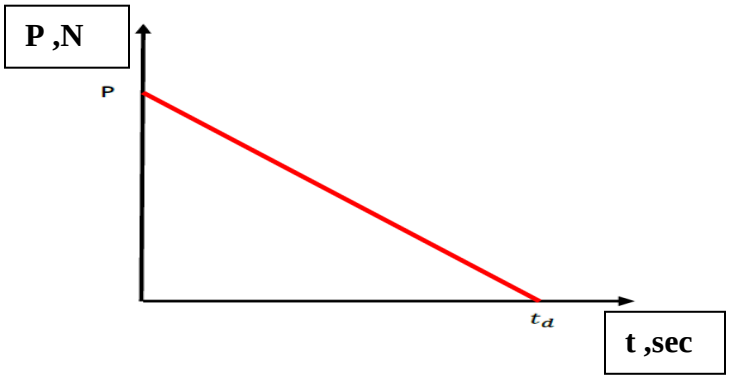

Figure 3- 3: Load- time relation in case of the triangular pulse loading conditions

From equation of motion :

$$m\ddot{x} + c\,\dot{x} + kx = 0 \qquad \text{……(3-13)}$$

$$\frac{p_1}{t_1} = \frac{\mathrm{p}(t)}{t_1-\tau} \qquad \text{…….(3-14)}$$

$$p_1(\tau) = \frac{p_1(t_1-\tau)}{t_1} \qquad \text{……(3-15)}$$

$$\mathrm{p}(\tau) = \left[\frac{p_1 * t_1}{t_1}\right] - \left[\frac{p_1 * \tau}{t_1}\right] = \left[1 - \frac{\tau}{t_1}\right] p_1 \qquad \text{……(3-16)}$$

$$x = \int_0^t e^{-\gamma\, \omega_n (t-\tau)} * \sin[\bar{\omega}(t-\tau)]\, \frac{p(\tau) d\tau}{m\, \bar{\omega}} \qquad \text{…….(3-17)}$$

but for the c = 0 the $\bar{\omega} = \omega_n \; and \; \gamma = 0$, $x = \int_0^t \sin[\omega_n (t-\tau)] * \frac{\left[1-\frac{\tau}{t_1}\right] p_1}{m\, \omega_n}\, d\tau$

$$x = \frac{p_1}{m\, \omega_n} \left[\int_0^t \sin[\omega_n (t-\tau)]\, d\tau - \frac{1}{t_1} \int_0^t \tau\, \sin[\omega_n (t-\tau)]\, d\tau\right] \qquad \text{…….(3-18)}$$

Assume u = τ , $d_u = 1 \; and \; d_v =$ $\sin[\omega_n (t-\tau)]\, d\tau$, $v = \frac{\cos \omega_n (t-\tau)}{\omega_n^2}$

$$\therefore x = \frac{p_1}{m\, \omega_n} \left[\left[\frac{\cos \omega_n (t-\tau)}{\omega_n}\right]_0^t - \frac{1}{t} \left[\left[\frac{\tau}{\omega_n} \cos \omega_n (t-\tau)\right]_0^t - \left[\frac{-\sin \omega_n (t-\tau)}{\omega_n^2}\right]_0^t\right]\right] \text{…(3-19)}$$

$$x = \frac{p_1}{m\, \omega_n} \left[\left[\frac{1}{\omega_n} - \frac{\cos \omega_n\, t}{\omega_n}\right] - \frac{1}{t} \left[\left[\frac{\tau}{\omega_n}\, (1-0)\right] - \left[0 - \frac{-\sin \omega_n\, t}{\omega_n^2}\right]\right]\right] \qquad \text{……...(3-20)}$$

$$x = \frac{p_1}{m\, \omega_n} \left[\frac{(1-\cos \omega_n\, t)}{\omega_n} - \frac{\tau}{\omega_n\, t} + \frac{\sin \omega_n\, t}{\omega_n^2}\right] = \frac{p_1}{m\, \omega_n^2} \left[1 - \cos(\omega_n\, t) + \frac{\sin(\omega_n\, t)}{t_1\; \omega_n} - \frac{\tau}{t_1}\right] \qquad \text{.. …(3-21)}$$

$$\therefore x_d = \frac{p_1}{K} [1 - \cos(\omega_n\, t)] + \frac{p_1}{K\, t_1} \left[\frac{\sin(\omega_n\, t)}{\omega_n} - t\right] \text{ for } t \le t_1 \qquad \text{…..(3-22)}$$

$$x_s = \frac{p_1}{K}$$

$$D.L.F = \frac{x_d}{x_s} = [1 - \cos(\omega_n\, t)] + \left[\frac{\sin(\omega_n\, t)}{\omega_n} - t\right] \frac{t}{t_1} \text{ for } t \le t_1 \qquad \text{....(3-23)}$$

for $t \ge t_1$, $c = 0$ in the case of freevibration

$x = A_1 \sin(\omega_n(t - t_1) + A_2 \cos(\omega_n(t - t_1), in\ the\ case\ of\ t = t_d$ .....(3-24)

$x^{\circ} = A_1\omega_n \cos(\omega_n(t - t_1) - A_2\omega_n \sin(\omega_n(t - t_1)$ ……(3-25)

Otherwise, for $t \le t_1$, $and\ x = \frac{p_1}{K}[1 - \cos(\omega_n t)] + \frac{p_1}{K\,t}\left[\frac{\sin(\omega_n t)}{\omega_n} - t\right]$ …. (3-26)

$x^{\circ} = \frac{p_1}{K}\left[\omega_n \sin(\omega_n t) + \frac{\cos(\omega_n t)}{t_1\,\omega_n^2} - \frac{1}{t_1}\right]$ and in order to find both of

$A_1$and A_2 let t = t_1 and,

$$x_{free\ vibration} = x_{triangular}\ ,\quad \overset{\circ}{x}_{free\ vibration} = \overset{\circ}{x}_{triangular}$$

$$\frac{p_1}{K}[1 - \cos(\omega_n t)] + \frac{p_1}{K\,t}\left[\frac{\sin(\omega_n t)}{\omega_n} - t\right] = A_1 * 0 + A_2 * 1$$

$$\therefore A_2 = \frac{p_1}{K}[1 - \cos(\omega_n t)] + \frac{p_1}{K\,t}\left[\frac{\sin(\omega_n t)}{\omega_n} - t\right]$$ .....(3-27)

$\left[-\omega_n \sin(\omega_n t_1) + \frac{\cos(\omega_n t)}{t_1\,\omega_n^2} - \frac{1}{t_1}\right] = A_1\,\omega_n * 1$, substitution the A_1 & A_2 in

$x_{free\ vibration}$

$x^{\circ} = \frac{p_1}{K\,\omega_n}\left[\omega_n \sin(\omega_n t) + \frac{\cos(\omega_n t)}{t_1\,\omega_n^2} - \frac{1}{t_1}\right] * \sin[\omega_n(t - t_1)] + \frac{p_1}{K}\left[(1 -\right.$

$\left.\cos(\omega_n t_1) + (\sin\frac{\sin(\omega_n t_1)}{\omega_n t_1} - \frac{t}{t_1})\cos(\omega_n(t - t_1)\right]$ ……. (3-28)

$$x^{\circ} = \frac{p_1}{K}\ [\sin(\omega_n\ t_1)\sin((\omega_n(t-t_1)) - \cos(\omega_n\ t_1)\ \cos((\omega_n(t-t_1))] +$$

$$\frac{p_1}{K\ \omega_n\ t_1}\ [\cos(\omega_n\ t_1)\sin((\omega_n(t-t_1)) + \sin(\omega_n\ t_1)\ \cos((\omega_n(t-t_1)) -$$

$$\sin((\omega_n(t-t_1))\ ] \qquad \text{……...(3-29)}$$

$$\therefore\ x_d = \frac{p_1}{K\ \omega_n\ t_1}\ [\sin(\omega_n\ t_1) - \sin((\omega_n(t-t_1))\ ] - \frac{p_1}{K}\ [\cos(\omega_n\ t_1)\ ] \quad \text{…..(3-30)}$$

and , $x_s = \frac{p_1}{K}$ therefore,

$$D.L.F = \frac{1}{\omega_n\ t_1}\ [\sin(\omega_n\ t_1) - \sin((\omega_n(t-t_1))\ ] -\ [\cos(\omega_n\ t_1)\ ] \quad \text{…..(3-31)}$$

for $t\ \geq t_1$

- **Symmetrical triangular pulse**

Consider now a symmetrical triangular pulse which starts at zero and reaches a maximum at one-half the total duration Figure 3- 4 .

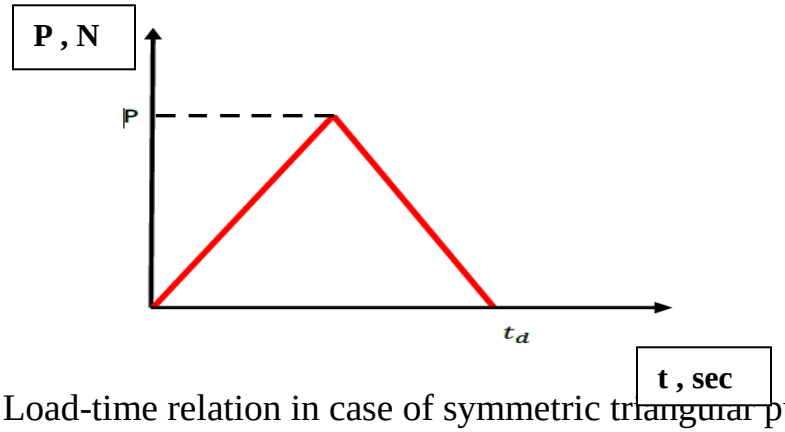

Figure 3- 4: Load-time relation in case of symmetric triangular pulse loading condition.

From equation of motion :

$$m\ddot{x} + c\,\dot{x} + kx = 0 \qquad \text{…….(3-32)}$$

$$\frac{p_1}{(t_1/2)} = \frac{p_{(\tau)}}{\tau}\,, \qquad 2\tau\,.p_1 = p_{(\tau)}\,.t_1\,, \qquad p_{(\tau)} = \frac{2\tau}{t_1}\,p_1\,, for\ 0 \le t \le t_1/2$$

$$x = \int_0^t e^{-\gamma\,\omega_n(t-\tau)} \sin\left[\bar{\omega}(t-\tau)\frac{p_\tau d\tau}{m\,\bar{\omega}}\right], \text{for } c = 0, \gamma = 0 \text{ and } \omega_n = \bar{\omega}$$

$$x = \int_0^t \sin\omega_n(t-\tau)\frac{2\,\tau\,p_1}{m\,\omega_n t_1}d_\tau = \frac{2\,p_1}{m\,\omega_n t_1}\int_0^t \sin\big(\omega_n(t-\tau)\big) * \tau * d_\tau \quad \text{…..(3-33)}$$

$$\text{assume}, u = \tau, d_u = 1 \text{ and } d_v = \sin\big(\omega_n(t-\tau)\big)\,, v = \frac{\cos\omega_n(t-\tau)}{\omega_n}$$

$$x = \frac{2p_1}{m\,\omega_n t_1}\left[\tau * \frac{\cos\omega_n(t-\tau)}{\omega_n}\right]_0^t - \left[\frac{-\sin\big(\omega_n(t-\tau)\big)}{\omega_n^2}\right]_0^t$$

$$x = \frac{2p_1}{m\,t_1\omega_n^2}\left[t - \frac{\sin\omega_n t}{\omega_n}\right], \qquad x = \frac{2p_1}{k\,t_1}\left[t - \frac{\sin\omega_n t}{\omega_n}\right] \qquad \text{…….(3-34)}$$

$$and\ for\ 0 \le t \le t_1$$

$$DLF = \frac{2}{t_1}\left[t - \frac{\sin\omega_n t}{\omega_n}\right] \qquad \text{……(3-35)}$$

$$\text{, for } \quad \frac{t_1}{2} \le t \le t_1\,, \qquad \frac{p_1}{t_1 - \frac{t_1}{2}} = \frac{p_{(\tau)}}{t_1 - \tau}$$

$$p_{(\tau)} = \left(1 - \frac{\tau}{t_1}\right)2p_1\,, \qquad x = \int_{\frac{t_1}{2}}^t \sin\omega_n(t-\tau) * \frac{\left(1 - \frac{\tau}{t_1}\right)2p_1}{m\omega_n}\,d\tau$$

$$x = \frac{2p_1}{m\omega_n}\left[\int_{\frac{t_1}{2}}^{t} \sin\omega_n(t-\tau)\ d\tau - \frac{1}{t_1}\int_{\frac{t_1}{2}}^{t} \tau\ \sin\omega_n(t-\tau)d\tau\right] \quad \text{.....(3-36)}$$

$$x = \frac{2p_1}{m\omega_n}\left[\left[\frac{\cos\omega_n(t-\tau)}{\omega_n}\right]_{\frac{t_1}{2}}^{t} - \frac{1}{t_1}\left[\frac{\tau}{\omega_n}\cos\omega_n(t-\tau)\right]_{\frac{t_1}{2}}^{t} - \left[\frac{-\sin\omega_n(t-\tau)}{\omega_n^2}\right]_{\frac{t_1}{2}}^{t}\right]$$

$$x = \frac{2p_1}{k}\left[\left[1-\cos\omega_n(t-\frac{t_1}{2})\right] - \frac{t}{t_1} - \left[\frac{1}{2}\cos\omega_n\left(t-\frac{t_1}{2}\right)\right] + \left[\frac{1}{t_1\omega_n}\sin\omega_n\left(t-\frac{t_1}{2}\right)\right]\right]$$

$$x = \frac{2p_1}{k}\left[1-\frac{1}{2}\cos\omega_n\left(t-\frac{t_1}{2}\right) - \frac{t}{t_1} + \frac{1}{t_1\omega_n}\sin\omega_n\left(t-\frac{t_1}{2}\right)\right] \quad \text{……(3-37)}$$

$$x_c = A_1\ \sin\omega_n\left(t-\frac{t_1}{2}\right) + A_2\ \cos\omega_n\left(t-\frac{t_1}{2}\right) \quad \text{…..(3-38)}$$

$$and\ x = x_c + x_p$$

$$x = A_1\ \sin\omega_n\left(t-\frac{t_1}{2}\right) + A_2\ \cos\omega_n\left(t-\frac{t_1}{2}\right) + \frac{2p_1}{k}\left[1-\frac{1}{2}\cos\omega_n\left(t-\frac{t_1}{2}\right) - \frac{t}{t_1} + \frac{1}{t_1\omega_n}\sin\omega_n\left(t-\frac{t_1}{2}\right)\right] \quad \text{……(3-39)}$$

$$x^{\circ} = A_1\ \cos\omega_n\left(t-\frac{t_1}{2}\right) - A_2\ \sin\omega_n\left(t-\frac{t_1}{2}\right)\omega_n + \frac{2p_1}{k}\left[0-\frac{1}{2}\sin\omega_n\left(t-\frac{t_1}{2}\right) - \frac{1}{t_1} + \frac{1}{t_1}\cos\omega_n\left(t-\frac{t_1}{2}\right)\right]\ for\ 0 \le t \le \frac{t_1}{2} \quad \text{……(3-40)}$$

$$x = \frac{2p_1}{kt_1}\left[t - \frac{\sin\omega_n t}{\omega_n}\right]\ and \quad \text{.. ……(3-41)}$$

$$x^{\circ} = \frac{2p_1}{kt_1}[1-\cos\omega_n t\ ] \quad \text{…….(3-42)}$$

therfore it can be observed that :

$x\ for\ 0 \le t \le \frac{t_1}{2}$ are equal to the x for $\frac{t_1}{2} \le t \le t_1$

$$\therefore A_2 = \frac{2p_1}{kt_1}\left[\frac{t_1}{2} - \frac{\sin \omega_n \frac{t_1}{2}}{\omega_n}\right] \quad \text{…. ..…..(3-43)}$$

and simmilar concept can be applied on x˚ to find A_1

$$\therefore A_1 = \frac{2p_1}{k\omega_n t_1}\left[1 - \cos \omega_n \frac{t_1}{2}\right] \quad \text{…..…..(3-44)}$$

$$x = \frac{2p_1}{k\omega_n t_1}\left[\left(1 - \cos \omega_n \frac{t_1}{2}\right) * \sin \omega_n \left(t - \frac{t_1}{2}\right)\right] + \frac{2p_1}{kt_1}\left[\left(\frac{t_1}{2} - \frac{\sin \omega_n \frac{t_1}{2}}{\omega_n}\right) *\right.$$

$$\left.\left(\cos \omega_n \left(t - \frac{t_1}{2}\right)\right)\right] - \left[\frac{t}{t_1} + \frac{1}{t_1 \omega_n} \sin \omega_n \left(t - \frac{t_1}{2}\right)\right] \quad \text{……(3-45)}$$

$$x = \frac{2p_1}{k\omega_n t_1}\left[\frac{1}{\omega_n}\sin \omega_n \left(t - \frac{t_1}{2}\right) - \frac{(\cos \omega_n \frac{t_1}{2}) * (\sin \omega_n \left(t - \frac{t_1}{2}\right))}{\omega_n}\right.$$

$$+ \frac{t_1}{2} \cos \omega_n \left(t - \frac{t_1}{2}\right) - \frac{(\sin \omega_n \frac{t_1}{2}) * (\cos \omega_n \left(t - \frac{t_1}{2}\right)}{\omega_n} + t_1$$

$$\left. - \frac{t_1}{2} \cos \omega_n \left(t - \frac{t_1}{2}\right) - t + \frac{1}{\omega_n}\sin \omega_n \left(t - \frac{t_1}{2}\right)\right]$$

$$\therefore x = \frac{2p_1}{kt_1}\left[t_1 - t - \frac{\sin \omega_n t}{\omega_n} + \frac{2}{\omega_n}\sin \omega_n \left(t - \frac{t_1}{2}\right)\right] \quad \text{……(3-46)}$$

$$\therefore D.L.F = \frac{2}{t_1}\left[t_1 - t - \frac{\sin\omega_n t}{\omega_n t} + \frac{2}{\omega_n}\sin\omega_n\left(t - \frac{t_1}{2}\right)\right] \quad \text{.....(3-47)}$$

in case of the free vibration , $t \geq t_1$

$x = A_1 \sin\omega_n(t - t_1) + A_2 \cos\omega_n(t - t_1)$, and when $t = t_1$, $A_2 = x$

at $\frac{t_1}{2} \leq t \leq t_1$

$$A_2 = \frac{2p_1}{kt_1}\left[t_1 - t - \frac{\sin\omega_n t}{\omega_n} + \frac{2}{\omega_n}\sin\omega_n\left(t - \frac{t_1}{2}\right)\right] = \frac{2p_1}{kt_1}\left[\frac{-\sin\omega_n t_1}{\omega_n} + \frac{2}{\omega_n}\sin\omega_n\frac{t_1}{2}\right] \quad \text{.....(3-48)}$$

simmlar concept to find the A_1 *, and the* $A_1 = x^{\circ}$ *at* $(\frac{t_1}{2} \leq t \leq t_1)$

$$A_1 = x^{\circ} = \frac{2p_1}{k\omega_n t_1}\left[0 - 1 - \cos\omega_n t_1 + 2\cos\omega_n\left(t - \frac{t_1}{2}\right)\right] \quad \text{.....(3-49)}$$

$$A_1 = \frac{2p_1}{k\omega_n t_1}\left[-1 - \cos\omega_n t_1 + 2\cos\omega_n\left(t - \frac{t_1}{2}\right)\right] \rightarrow \therefore x = \frac{2p_1}{k\omega_n t_1}\left[-1 - \cos\omega_n t_1 + 2\cos\omega_n\left(t - \frac{t_1}{2}\right)\right] *$$

$$\sin\omega_n(t - t_1) + \frac{2p_1}{kt_1}\left[\frac{-\sin\omega_n t_1}{\omega_n} + \frac{2}{\omega_n}\sin\omega_n\frac{t_1}{2}\right] * \cos\omega_n(t - t_1) \quad \text{.....(3-50)}$$

$$\therefore x = \frac{2p_1}{k\omega_n t_1}\left[2\sin\omega_n\left(t - \frac{t_1}{2}\right) - \sin\omega_n t - \sin\omega_n(t - t_1)\right] \quad \text{.....(3-51)}$$

$$\therefore DLF = \frac{2}{\omega_n t_1}\left[2\sin\omega_n\left(t - \frac{t_1}{2}\right) - \sin\omega_n t - \sin\omega_n(t - t_1)\right] \quad \text{.....(3-52)}$$

- **Constant force with finite rise time**

A force can never be applied instantaneously , it is of interest to investigate a loading which has a finite rise time but remains constant thereafter as shown in Figure 3- 5 .

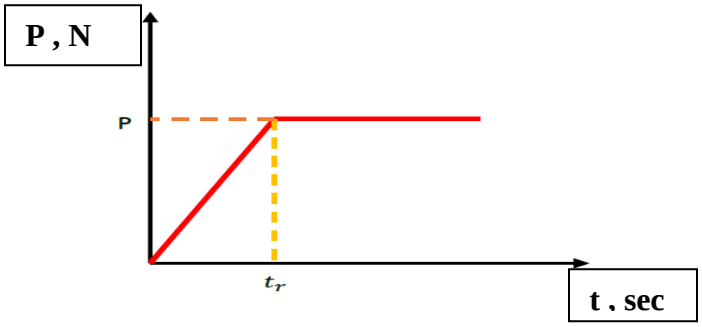

Figure 3- 5: Load-time relation in case of the constant pulse loading condition

$$\frac{p_1}{t_r} = \frac{p_{(\tau)}}{\tau} \rightarrow p_\tau = \frac{\tau}{t_r} p_1 \qquad \text{……(3-53)}$$

$$x = \int_0^t e^{-\gamma\, \omega_n (t-\tau)} \sin\left[\bar{\omega}(t-\tau)\frac{p_\tau d\tau}{m\,\bar{\omega}}\right] \qquad \text{…….(3-54)}$$

for $c = 0, \gamma = 0$ and $\omega_n = \bar{\omega}$

$$x = \int_0^t \sin \omega_n (t-\tau)\frac{p_1}{m\,\omega_n t_r} d_\tau = \frac{p_1}{m\,\omega_n t_r}\int_0^t \sin\left(\omega_n (t-\tau)\right) * \tau d_\tau$$

$$\text{assume}, u = \tau, d_u = d_\tau \text{ and } d_v = \sin\left(\omega_n (t-\tau)\right), v = \frac{\cos \omega_n (t-\tau)}{\omega_n}$$

$$x = \frac{p_1}{m\,\omega_n t_r}\left[\tau * \frac{\cos \omega_n (t-\tau)}{\omega_n}\right]_0^t - \left[\frac{-\sin\left(\omega_n (t-\tau)\right)}{\omega_n^2}\right]_0^t = \frac{p_1}{m\,\omega_n t_r}\left[(t-0) - \left(\frac{t_1}{\omega_n}\sin(\omega_n . t)\right)\right]$$

$$x = \frac{p_1}{m\,\omega_n t_r}\,[t - \sin(\omega_n . t)\,] \qquad \text{.....(3-55)}$$

$$\text{and} \quad \boldsymbol{D.L.F} = \frac{1}{t_r}\,[t - \sin(\omega_n . t)\,] \text{ for } 0 \le t \le t_r \qquad \text{.....(3-56)}$$

$for\ t \ge t_r\ for\ find\ \ x_p\ and\ p_1 = p_{(\tau)}$

$$x_p = \int_{t_r}^{t} (\sin \omega_n . (\,t - \tau)) * \frac{p_\tau}{m\,\omega_n}\, d_\tau \qquad \text{.....(3-57)}$$

$$x_p = \frac{p_1}{m\,\omega_n} \int_{t_r}^{t} (\sin \omega_n . (\,t - \tau))\, d_\tau \ , \quad x_p = \frac{p_1}{m\,\omega_n^2}\,[\cos \omega_n . (\,t - \tau)]_{t_r}^{t}$$

$$x_p = \frac{p_1}{m\,\omega_n^2}\,[1 - \cos \omega_n . (\,t - t_r)\,] \qquad \text{.....(3-58)}$$

$and\ x = \ x_c + x_p$

$$x_c = A_1\ \sin \omega_n . (\,t - t_r) + \ A_2\ \cos \omega_n . (\,t - t_r) \qquad \text{.....(3-59)}$$

$$A_1 = \frac{p_1}{m\,\omega_n^3 t_r}\,[1 - \cos(\omega_n . t)], and\ A_2 = \frac{p_1}{m\,\omega_n^2 t_r}\left[t - \frac{\sin(\omega_n . t)}{\omega_n}\right]$$

$$A_1 = \frac{p_1}{m\,\omega_n^3 t_r}\,[1 - \cos(\omega_n .\ t_r)], \qquad and\ A_2 = \frac{p_1}{m\,\omega_n^2 t_r}\left[t_r - \frac{\sin(\omega_n . t_r)}{\omega_n}\right]$$

$$\therefore x = \frac{p_1}{m\,\omega_n^2}\,[1 - \cos \omega_n . (\,t - t_r)\,] + \left\{\frac{p_1}{m\,\omega_n^3 t_r}\,[1 - \cos(\omega_n .\ t_r)]\right\} \sin[\omega_n . (\,t -$$

$$t_r)] + \left\{\frac{p_1}{m\,\omega_n^2 t_r}\left[t_r - \frac{\sin(\omega_n . t_r)}{\omega_n}\right]\right\} \cos \omega_n . (\,t - t_r) \qquad \text{.....(3-60)}$$

$let\ k = m * \ \omega_n^2$

$$\therefore x = \frac{p_1}{k} + \frac{p_1}{k\,\omega_n t_r}\,[\sin[\omega_n . (\,t - t_r)] - \sin(\omega_n . t)\,] \qquad \text{.....(3-61)}$$

$$\therefore D.L.F = 1 + \frac{1}{\omega_n t_r}\,[\sin[\omega_n . (\,t - t_r)] - \sin(\omega_n . t)\,] \qquad \text{.....(3-62)}$$

Table (3-1) : Equations of displacement for variable type of loads

Load	Displacement
Rectangular Pulse load	$x_{d_t} = \frac{p_\circ}{m\,\omega_n^2}\ (1-\cos\omega_n t)$ …….force $x_d = \frac{p_\circ}{K}\left[\cos(\omega_n (t-t_1)) - \cos(\omega_n t)\right]$ …….free
Triangular Pulse load	$x_d = \frac{p_1}{K}\ [1-\cos(\omega_n t)] + \frac{p_1}{K\,t_1}\left[\frac{\sin(\omega_n t)}{\omega_n} - t\right]$ ..force $x_d = \frac{p_1}{K\,\omega_n\,t_1}\ [\sin(\omega_n t_1) - \sin((\omega_n(t-t_1))\,] -$ $\frac{p_1}{K}\ [\cos(\omega_n t_1)\,]$ ….. free
Symmetrical triangular pulse Symmetrical triangular pulse	$x = \frac{2p_1}{kt_1}\left[t_1 - t - \frac{\sin\omega_n t}{\omega_n} + \frac{2}{\omega_n}\sin\omega_n\left(t-\frac{t_1}{2}\right)\right]$ force $x = \frac{2p_1}{k\omega_n t_1}\left[2\sin\omega_n\left(t-\frac{t_1}{2}\right) - \sin\omega_n t - \sin\omega_n(t-t_1)\right]$ …… free
Constant force with finite rise time	$x = \frac{p_1}{m\,\omega_n t_r}\ [t - \sin(\omega_n . t)\,]$ …….force $x = \frac{p_1}{k} + \frac{p_1}{k\,\omega_n t_r}\ [\sin[\omega_n .(\,t-t_r)] - \sin(\omega_n . t)\,]$ free

3.2.2 Elastoplastic Material Model

Regarding the word, elastoplastic is the state of the material that shows both elastic behaviours till it exceeds the elastic limit and then is stretched to show plastic behaviour without any apparent defects. As such it's the region between elastic point and yield point is known as the Elastoplastic region. In ductile materials (like mild steel) this elastoplastic region is large as compared to brittle materials(concrete). In this region material is partial elastic and partial plastic. It means if the material is loaded up to its Elastoplastic region, then the material will not recover its whole deformation. Elastic Limit-point up to which material shows elastic behaviour while the Yield Point- material starts going into a plastic state. From the deformation point of view, the elastic body is able to return to the original shape (thus, there is no residual deformation) after unloading. If there is some remaining deformation after the force is removed - this is plastic deformation. Usually, the deformation is elastic for small stresses/strains. Smoothly becomes plastic for greater stresses (we actually have to assume some conventions to draw a borderline between these two types) and in the end, the stress will overcome the material strength and the sample breaks. Therefore, studying this stage is giving an acceptable understanding of the structural element failure.

- **Rectangular Pulse Load**

$$x = \frac{p_\circ}{m\omega_n^2}\,(1 - \cos\omega_n\, t) \qquad \text{.....(3-63)}$$

$$x = \frac{p_\circ}{m\,\omega_n}\,(1 - \cos\omega_n\, t) \quad \text{and } x_{static} = \frac{p_\circ}{K} \qquad \text{.....(3-64)}$$

$since\ the\ p_\circ = K * x$

$\therefore x = x_{static}\,(1 - \cos(\omega_n t))\,,\ 0 \le t \le t_{el}$ for the elastic range .....(3-65)

in the case of $t = t_{el}\,, x = x_{el}\,,$

$x = x^{\circ} = x_{static} * \omega_n * \sin(\omega_n t_{el})$

and the time when x_{el} is reached is

$\cos(\omega_n t_{el}) = \left[1 - \frac{x_{el}}{x_{static}}\right]$ .....(3-66)

and let $t_1 = t - t_{el}$

for the intial conditions $t_1 = 0\,,\quad t = t_{el}$ and the

$x^{\circ} = x_{static}\,\omega_n \sin(\omega_n t_{el})$ .....(3-67)

regarding equation of motion $m\ddot{y} + c\dot{y} + ky = p_{\circ}$ .....(3-68)

in the case of the plastic range $kx = Rm$

$m\ddot{x} + Rm = p_{\circ}$ .....(3-69)

$\ddot{x} = \frac{p_{\circ} - Rm}{m}$ .....(3-70)

$\dot{x} = \frac{1}{m}(p_{\circ} - Rm)t_1 + c_1$ .....(3-71)

$x = \frac{1}{2m}(p_{\circ} - Rm)t^2 + c_1 t_1 + c_2$ .....(3-72)

by applying the boundary conditions $t = t_{el}\,,$ at $t = 0$

$x_{el} = x_{from\ equation\ of\ motion}\, y_{static}(1 - \cos(\omega_n t_1)) = \frac{1}{2m}(p_{\circ} - Rm)t^2 + c_1 t_1 + c_2$

$\therefore\ c_2 = x_{el}, \text{and}\ x_{static} * \omega_n * \sin(\omega_n t_{el}) = \frac{1}{2m}(p_{\circ} - Rm)t_1^2 + c_1 t_1 + c_2$

$c_1 = x_{static}\,\omega_n * \sin(\omega_n t_{el})$

$\therefore x = \frac{1}{2m}\ (p_\circ - Rm)t^2 + \ x_{static}\ \omega_n * t_1 \sin(\omega_n\ t_{el}) + \ x_{el}$, for the $x_{el} \le x \le x_{max}$ …….(3-73)

$0 = \frac{2}{2m}\ (p_\circ - Rm)t_1 + x_{static}\ \omega_n \sin(\omega_n\ t_{el}) + \ 0$

$t_1 = \frac{m\ x_{static}\ \omega_n \sin(\omega_n\ t_{el})}{(\ Rm - p_\circ)}$ ……..(3-74)

and the ductility ratio is $\mu = \frac{x_{max}}{x_{el}}$

- **Triangular Pulse Load**

$x = \frac{p}{K}\ (1 - \cos\omega_n t) + \frac{p}{K+d}\left[\frac{\sin(\omega_n t)}{\omega_n} - t\right]$ ……(3-75)

$\dot{x} = \frac{p}{K}\ \omega_n \sin\omega_n t + \frac{p}{K+d}\ \cos(\omega_n t - 1)$ …….(3-76)

$\ddot{x} = \ \omega_n^2\ x_{st}\ \left[\cos(\omega_n t) - \ \frac{\sin(\omega_n t)}{td\omega_n}\right]$ ……..(3-77)

$m\ddot{x} + Rm = p(t)\ \rightarrow m\ \ddot{x} = \ p_1 \frac{(td - t)}{td} - Rm$

$\ddot{x} = \ \frac{p_1\ \left(1 - \frac{t}{td}\right)}{M} - Rm$

$\ddot{x} = \ \frac{1}{M}\left[p_1\ \left(1 - \frac{t_1}{td} - \ \frac{t_{el}}{td}\right) - Rm\right]$ …….(3-78)

$\dot{x} = \ \frac{1}{M}\left[p_1\left(t_1 - \frac{t_1^2}{2td} - \ \frac{t_{el}\ t_1}{td}\right) - Rm\ t_1\right] + \ c_1$ ……(3-79)

$x = \ \frac{t_1^2}{2M}\left[p_1\left(1 - \frac{t_1^3}{3td} - \ \frac{t_{el}}{td}\right) - Rm\ \right] + \ c_1 t_1 + \ c_2$ …….(3-80)

$t = \ t_{el}$ when $t_1 = 0$

and from the elastic stage $x = x_{el}$, $x_{(t=0)} = x_{(t=t_{el})}$

$\therefore c_2 = x_{elastic}$ ……(3-81)

while, for $t_1 = 0$, $\dot{x}_{(t_1=0)} = \dot{x}_{(t=t_{el}),}$, $c_1 = \dot{x}_{(t=t_{el})}$

$\dot{x}_{(t=t_{el})} = \omega_n x_{static} \sin(\omega_n t_{el}) + \frac{x_{static}}{td} [\cos(\omega_n t_{el}) - 1]$

$\dot{x}_{(t=t_{el})} = x_{static} \left[\omega_n \sin(\omega_n t_{el}) + \left(\frac{1}{td}\cos(\omega_n t_{el})\right) - 1\right]$ …..(3-82)

for $c_1 = \dot{x}_{(t=t_{el})}$

$and\ c_2 = x_{elastic} = x_{static}\ (1 - \cos(\omega_n t_{el}))$ ……(3-83)

$\therefore x =$

$\frac{t_1^2}{2M}\left[p_1\left(1 - \frac{t_1^3}{3td} - \frac{t_{el}}{td}\right) - Rm\right] + x_{static}\ t_1\left[\omega_n \sin(\omega_n t_{el}) + \left(\frac{1}{td}\cos(\omega_n t_{el})\right) - 1\right] + x_{static}\ (1 - \cos(\omega_n t_{el})) + \frac{x_{static}}{td}\left[\frac{\sin(\omega_n t)}{td\omega_n} - t_{el}\right]$ ……(3-84)

in order to evaluate $t_{1,max}\ the\ t_{el}\ \frac{d_x}{d_{t1}} = 0$

$\dot{x} = \frac{1}{2M}\left[p_1\left(2t_1 - \frac{t_1^2}{td} - \frac{t_{el}\ t_1}{td}\right) - 2\ t_1 Rm\right] + \dot{x}_{(t=t_{el})} = 0$

$p_1\left(2t_1 - \frac{t_1^2}{td} - \frac{t_{el}\ t_1}{td}\right) - 2\ t_1 Rm = -2M\ \dot{x}_{(t=t_{el})}$ …..(3-85)

3.3 Visual Basic programming

This part of chapter three reviews the dynamic analysis of the hollow-core slab by using **Visual Basic** language. In general, all of the eight forms have been utilized as well as prepared in a plain way for the easiest use of all tools in this

program. Solving the problems that need iterative attempts with acceptable accurate outcomes is hard to finish without the assistance of a computer which explains the need as well as existence for such programming languages like **Visual Basic**. Checking of the outcomes that obtained by **Visual Basic** language is done through the comparisons between the obtained outcomes with the finite element software results (**ABAQUS Standard/Explicit 2020**). Furthermore, a comparison between the present work and an application in **Structural Dynamics Handbook** (John M. Biggs), will be clarified in the application parts of chapter four.

3.3.1 Objectives of running Visual Basic programming

The main aims of using the **Visual Basic** programming language can be briefly listed as follows:

1. Establishing a dynamic analysis process for the hollow-core slab system (which is, our focus).
2. Building a **Visual Basic** user interface as a way of being scientifically productive for further future research studies.

3.3.2 Clarification of the program forms

The definition form of program consists of three minor command buttons (next, end, help) as shown in Plate 3- 1 , every button deals with a part of the main program and each of them share in between to solve the required problem. The equations that are mentioned in chapter three have been programmed in dynamic analysis buttons. After pressing on the command button (Next) that appear second form that is contain type of loading and hide this form of definition, and after pressing on the command button (End) that end the program, after pressing on the command button (Help) that show eight form.

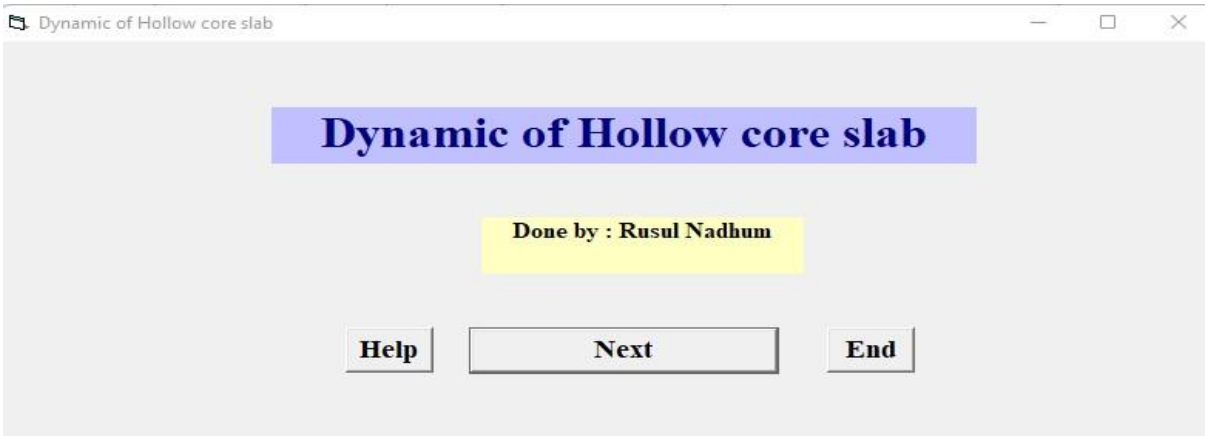

Plate 3- 1: Definition form of hollow core slab program

3.3.3 Type of loading (dynamic analysis) form

Dynamic loading (dynamic analysis) form will be responsible for the analysis of the hollow core slab as shown in Plate 3- 2. This form contains four option and each option responsible about choice the type of loading, and contain two command buttons (Next, Back). after pressing on the command button (Next) that appear form that contain the load pervious choice, while After pressing on the command button (Back) that appear pervious form.

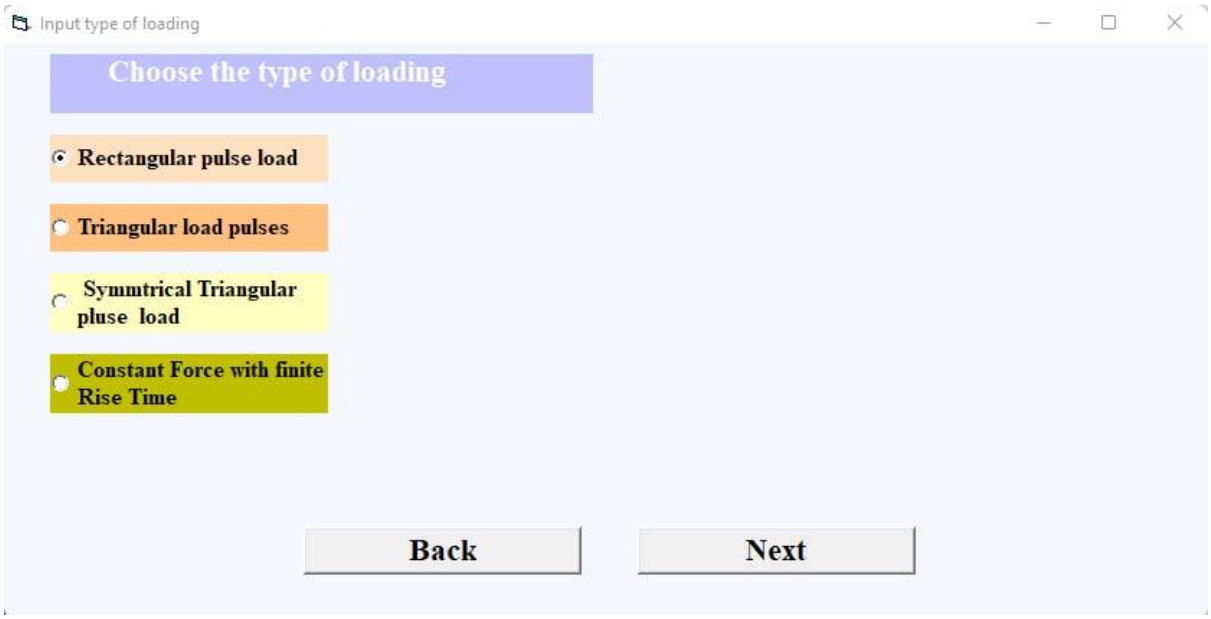

Plate 3- 2: Type of loading form of hollow core slab program

3.3.4 Section properties and selection the type of vibration button

After pressing on the button (Next) in pervious form, the form of section properties and choose the type of vibration appear as shown in Plate 3- 3 . It is used for choice the type of vibration from two options and entering the properties:

1. Plastic moment of hollow core slab (Rm).
2. Mass of hollow core slab (m).
3. Dynamic load (p).
4. Moment of inertia of Hollow core slab(I).
5. Modulus of elasticity of Hollow core slab(E).
6. Length of Hollow core slab (L).
7. Time duration (t).

This form also contain two main command button and three minor command button , this minor used to calculate some parameters such as (Rm, m, I) those symbols refer to (Plastic moment, mass, moment of inertia) respectively for hollow core slab by programmed the regulation concern to that symbols in this command button , and entering the properties of hollow core slab such as (length, width, thickness, radius of void, number of void, ……etc.) to calculate after pressing on those commands button. And when Pressing on the command button (Show the result) after completing the entering all the information will directly hide this form and appear next form that contain the result by programmed the equation in this command button, and when pressing on the command button (Back) hide this form and back to pervious form.

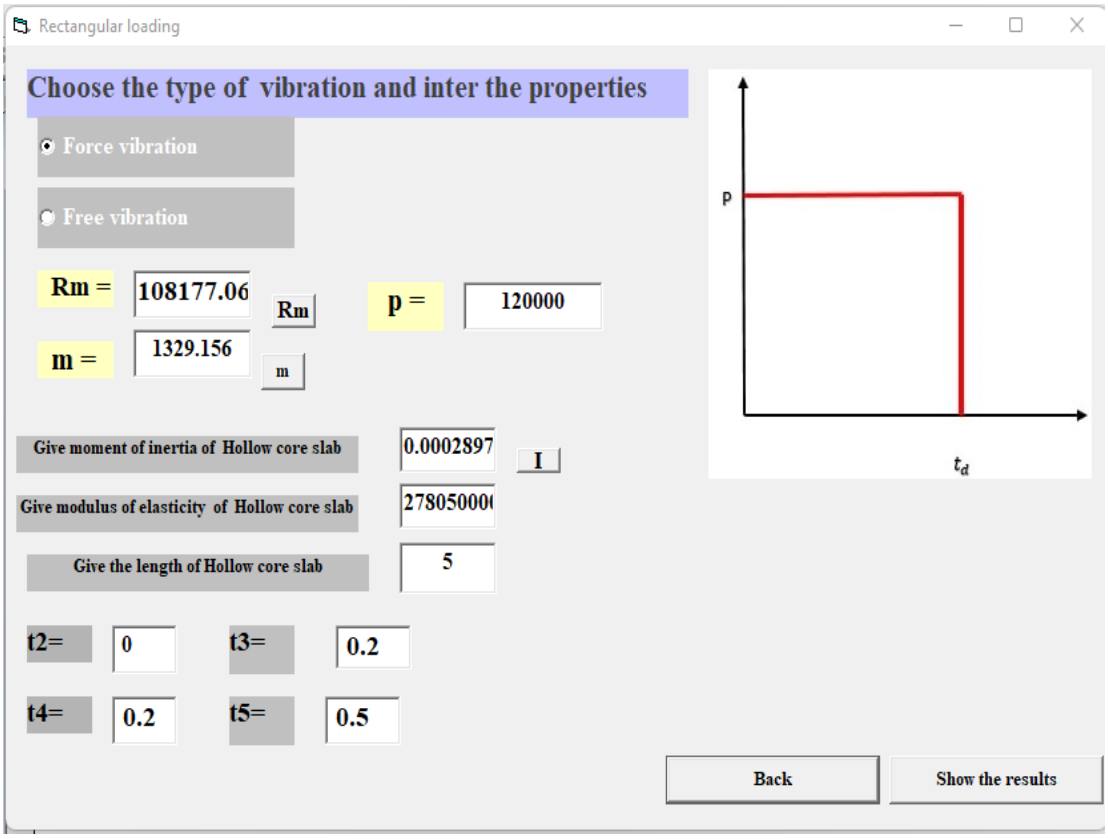

Plate 3- 3: Section properties and type of vibration form of hollow core slab program

When choose the second choice that is (triangular loading) would appear next form (form 4) as shown in Plate 3- 4 , is same to pervious form by choice type of vibration and entering properties, and when pressing on command button (show the results) would hide this form and appear form 7 (form results). Above pervious loads consist of two stage (elastic and elasto-plastic) range

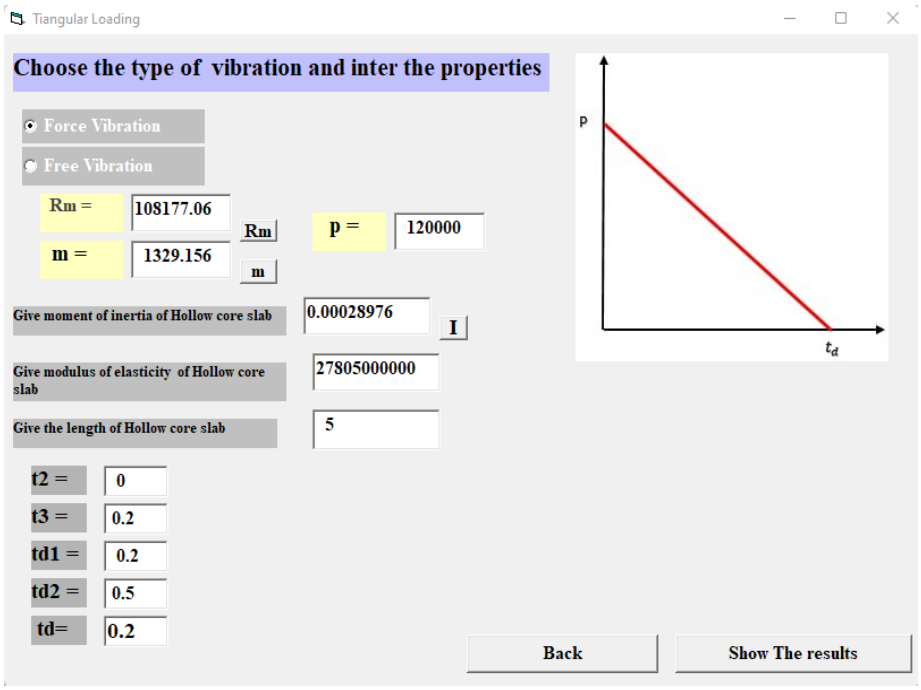

Plate 3- 4: Triangular loading form of hollow core slab program

And when pressing on three choices (symmetrical triangular loading) will appear next form (form 5) as shown in Plate 3- 5 , that concern to this choice contain command button programmed in it equations of this type load and when entering properties of hollow core and pressing on command button (show the results) will appear form 7 (form results).

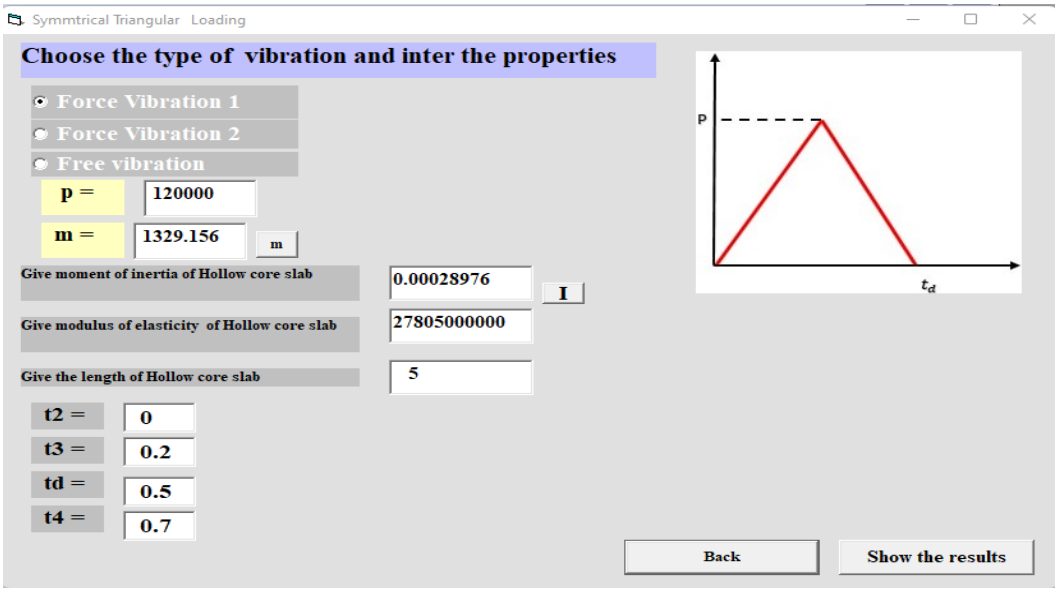

Plate 3-5: symmetrical Triangular loading form of hollow core slab program

And when choice four loading (constant loading) will appear form 6 as shown in Plate 3- 6 , concern to this load that contain type of vibration and properties of hollow core and some minor commands button use to calculate (m, I). And major commands button when pressing on (show the results) will appear form 7 (results form) and hide form 6 since it programmed to make this, and when pressing on command button (back) will hide form 6 and back to pervious form (form 5). Above pervious two loads (symmetrical triangular and constant) load programmed in elastic range only.

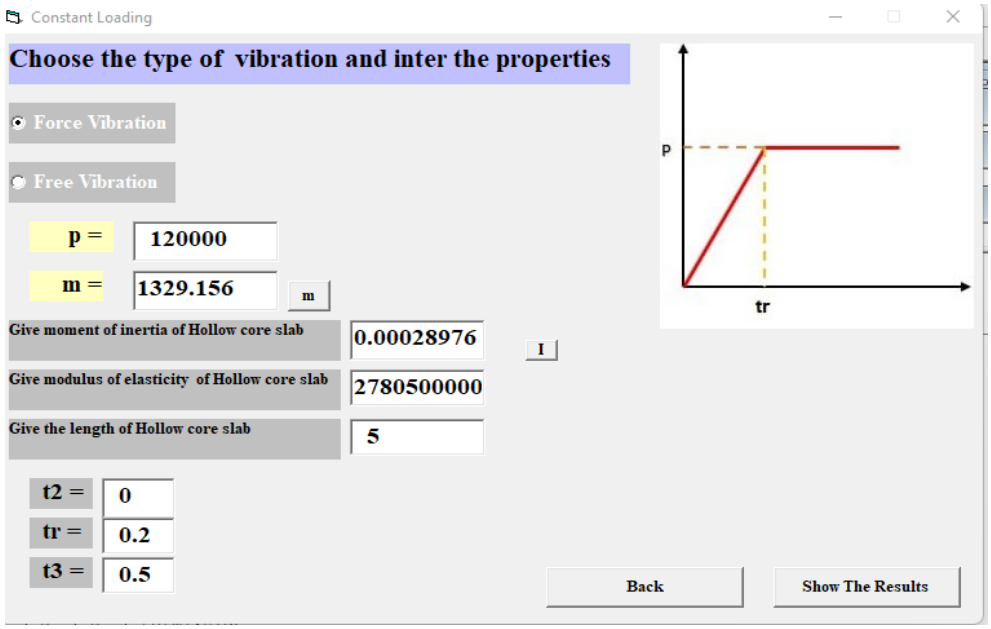

Plate 3-6: Constant loading form of hollow core slab program

3.3.5 Results form

when pressing on any command button its caption is (show the results) will appear this form as shown in Plate 3- 2 , contain results required such as (time, displacement, time of period, stiffness, frequency, static displacement, elastic displacement, time elastic, max time, max displacement and ductility ratio) and contain two commands button (Back, End), when pressing on (back) will back to pervious form and when pressing on (end) will stop the program.

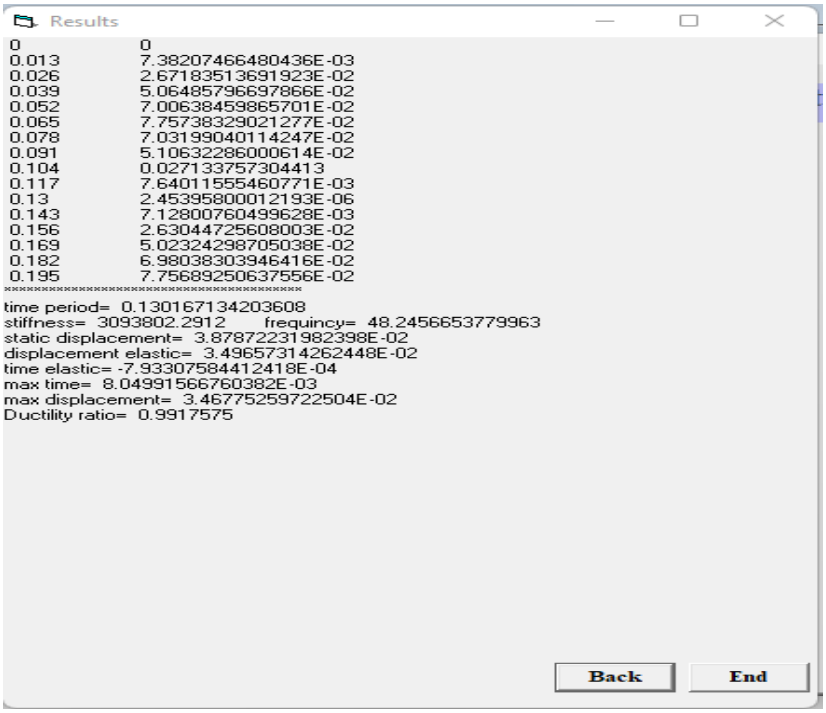

Plate 3- 7: Results form of hollow core slab program

3.3.6 Help form

When pressing on command button its caption is (help) in form 1 (definition form) will appear form 8 (help form) as shown in Plate 3- 8 , contain message tell user this program used to dynamic analysis of hollow core slab with four type of load.

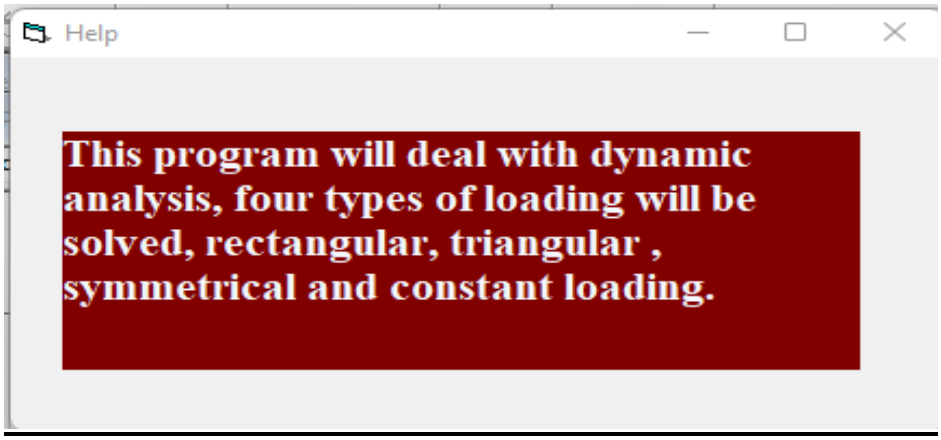

Plate 3-8: Help form of hollow core slab program

3.3.7 Operating the program

The following procedure is used for operating the program:

1. Press the type of load option.
2. press the type of vibration option and enter the information of section.
3. Press show the results button to make the required analysis for hollow core slab. This step cannot be done before any other steps as shown in flowchart Figure 3- 5 .

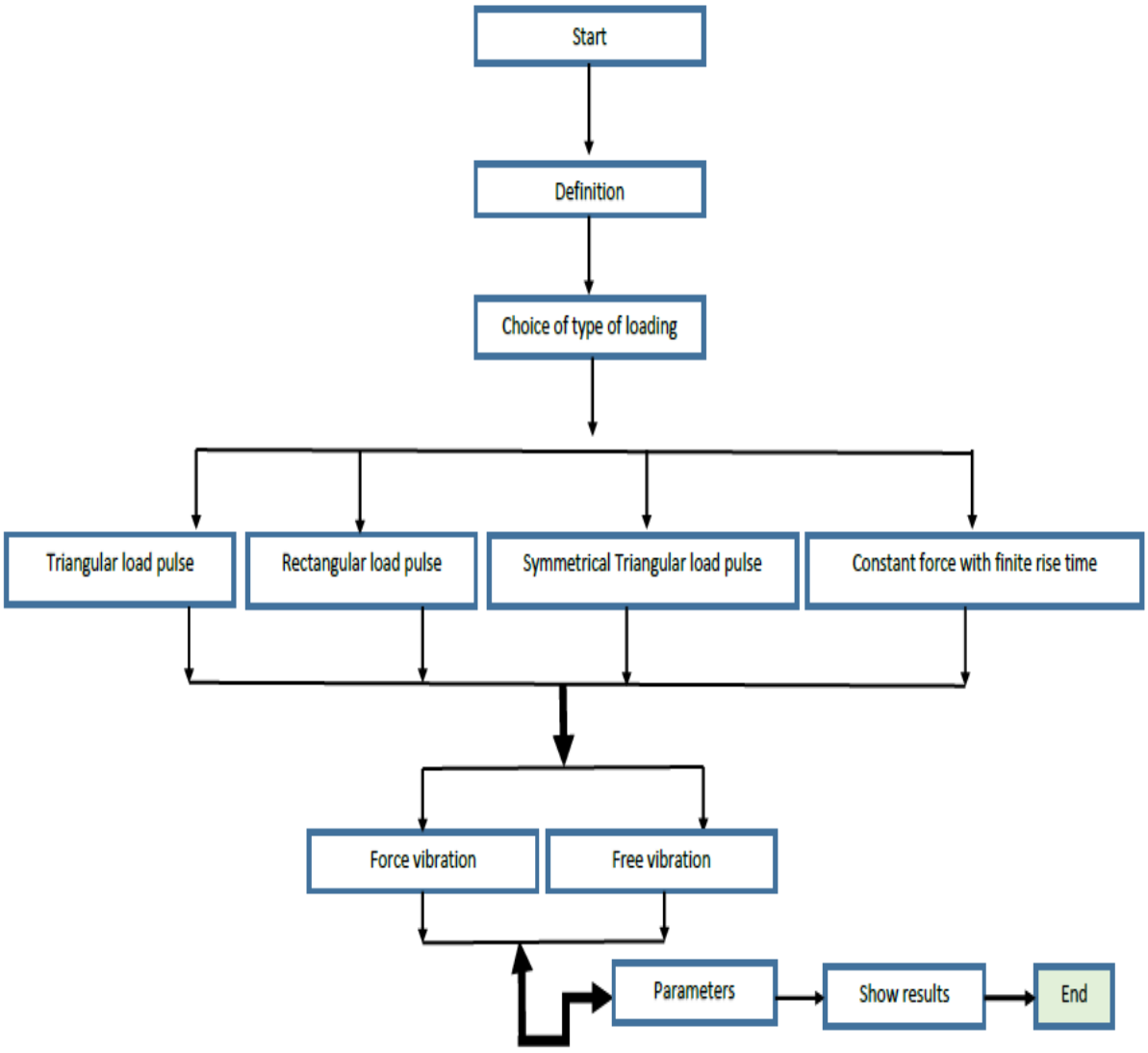

Figure 3- 6: Flow chart for operating the program

3.4 Numerical analysis using finite element software

The primary concern in this part of chapter three is to investigate the behaviour and dynamic load capacity of hollow-core slab under various loading conditions that are analytically discussed in previous sections. Using the **ABAQUS Standard/Explicit 2020** finite element model to visualize the failure modes of each model and its capacity in order to compare the results obtained by aforesaid software with the adopted analytical model.

3.4.1 Model geometric configuration and elements types

The geometric configuration of the hollow-core slab is drawn by using **Auto-Cad R2020** software and then exported into **ABAQUS Standard/Explicit 2020** later for carrying out the analysis. The properties of the hollow-core slab already drawn by **Auto-Cad R2020** are (L=5 m) slab length, (B= 1.2 m) slab width, (H=0.15 m) slab thickness, and Density = 24000 N/m3 , Number of void = 7 , Diameter = 0.1 m ,Ec = 27805 MPa , Es = 186165 MPa , Fpu = 1662 MPa , As= 2.34E-05 m, Ɛi = 0.005165

all specimens are modelled by **ABAQUS Standard/Explicit 2020** to study the dynamic load capacity and investigate the failure modes as well as behaviour of the hollow-core slab.

3.4.2 Parts and Assembly

The model of hollow-core slab model in this study consisted of substantial (concrete part and strands). The geometric configuration of this concrete part has been imported from the **Auto-Cad R2020** software and then represent the final shape of the hollow-core slab unit as shown in plate 3-9.

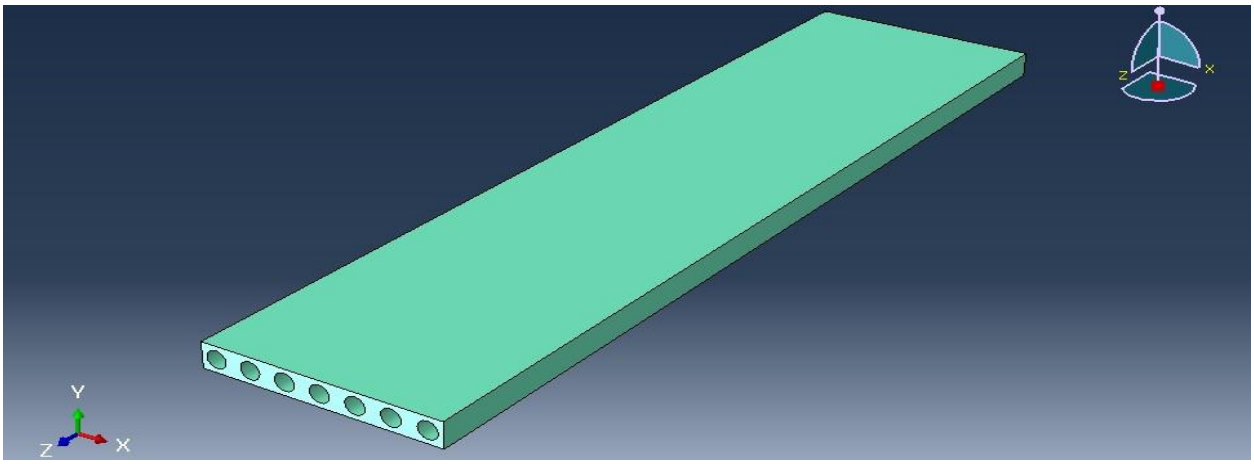

Plate 3- 9: The imported hollow-core slab model

And represent pre-stress as stress in strands as clarified below:-

$$Es = \frac{\sigma}{\epsilon}$$

3.4.3 Constitutive concrete material model properties

In general, three constitutive material models by **ABAQUS Standard/Explicit 2020** can be applied to simulate the behaviour of concrete material depending on the case that has to analyse. The concrete-smeared cracking model usually utilised to simulate behaviour of the concrete under standard static loading conditions. Meanwhile, the brittle cracking model is used for the most cases of only **Explicit- Dynamic** loading conditions. Eventually, the concrete damaged plasticity model which provide by **ABAQUS/Explicit** solver is capable

to consider both of the static as well as dynamic performance of concrete material which is selected in this study as can be observed in the Plate 3-10. Moreover, each one of aforesaid constitutive material models are capable to study behaviour of the material whether having embedded steel-reinforcements or even not.

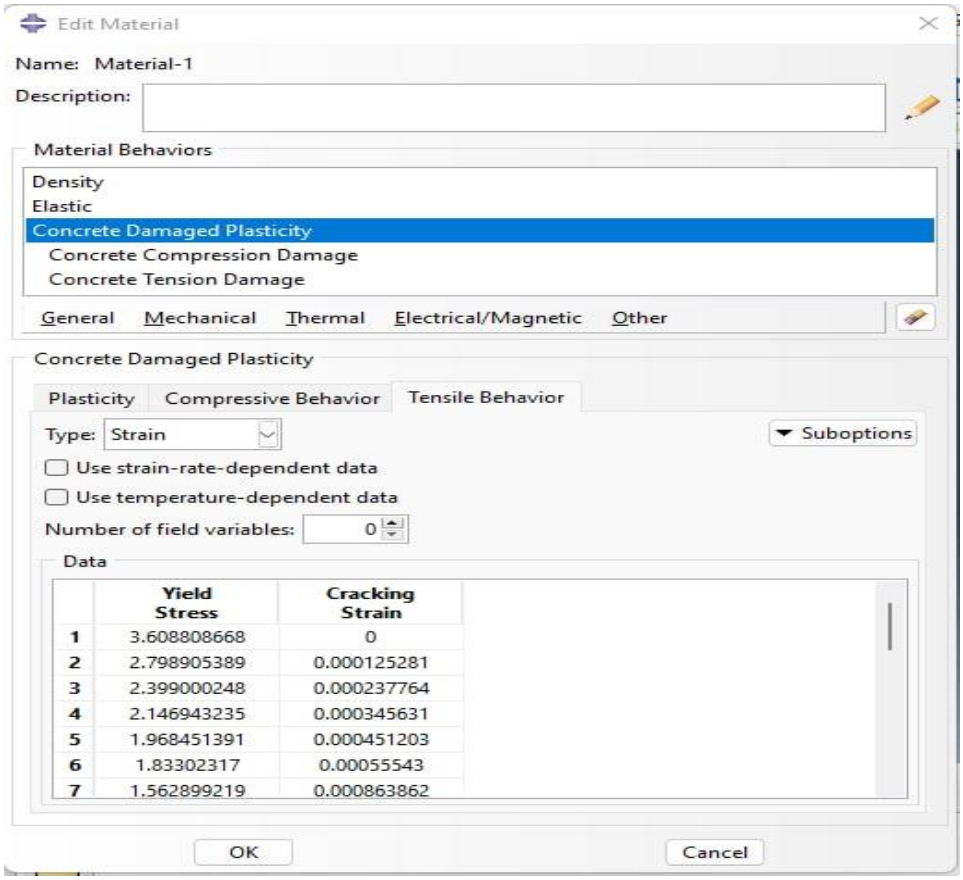

Plate 3-10: Selection of concrete damage plasticity model

The need for considering the degradation of the elastic stiffness that occurred due to plastic straining which can be observed in the Plate 3-11 which defined based on the data shown in Table 3-3 and Table 3-4, under arbitrary loading conditions either tension or compression is important for reliable simulation, and make the concrete damaged plasticity model are the acceptable choice for the such cases.

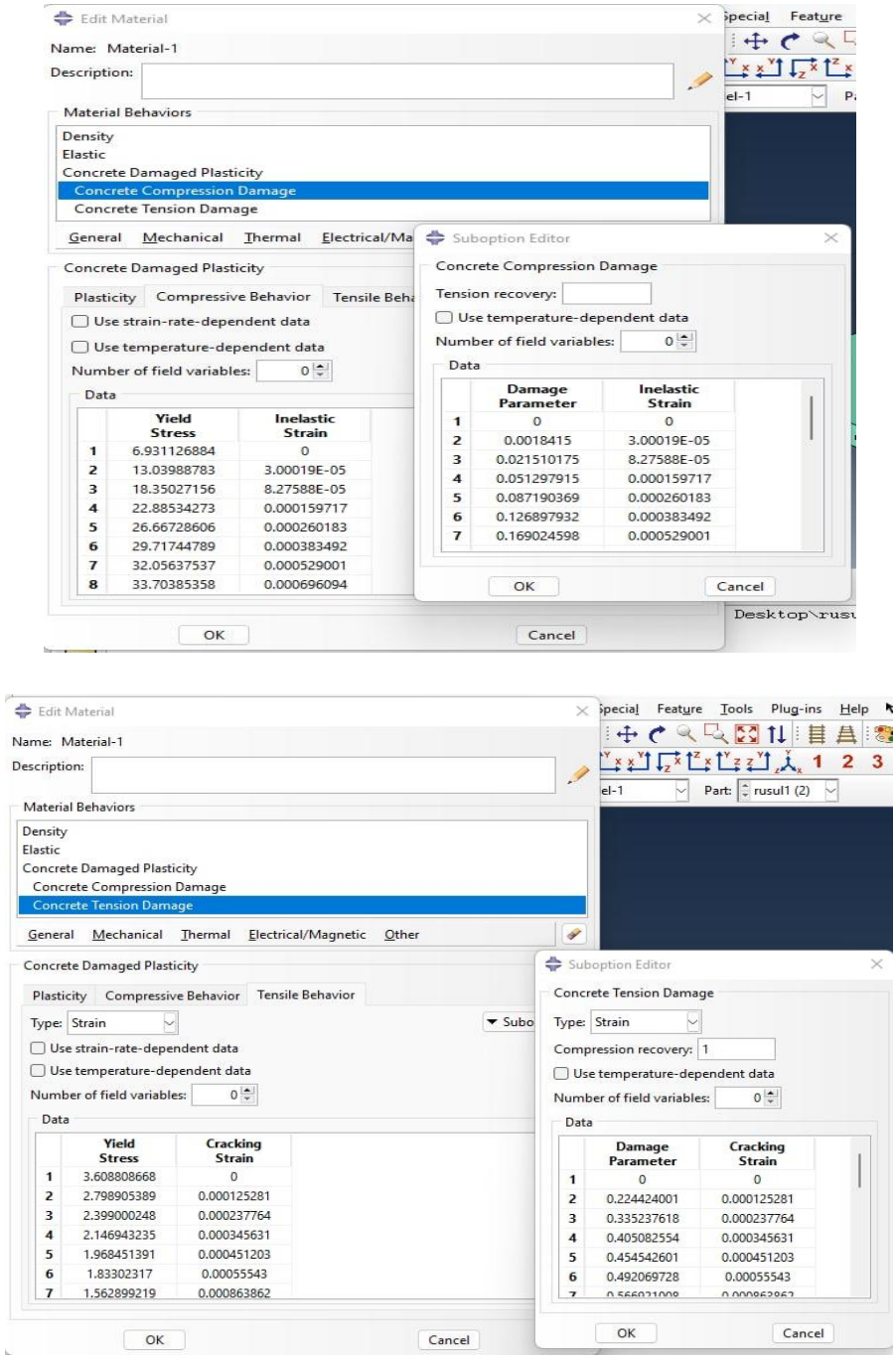

Plate 3-11: Selected compression and tension damage parameters of concrete

As such, many reasons can be briefly listed as following make the concrete damaged plasticity model is the unique choice for most complicated cases.

1. Applicate assumption for this model is the scalar (isotropic) damage which specially designed for arbitrary loading conditions which takes into account the influence of stiffness recovery.
2. In comparison with the smeared crack model, the concrete damaged plasticity model provides higher potential for convergence.
3. The concrete damaged plasticity model provides different yield strength for both of compression and tension as can be noticed in the Plate 3-13.
4. The concrete damaged plasticity model provides different degradation of the elastic stiffness for both of compression and tension as clearly shown in the Plate 3-12 and Plate 3-13.
5. The true post yield (plastic) response for instance softening behaviour in tension instead of initial hardening then followed later by softening which can be considered only by this constitutive model.

The property of the concrete material utilised in this research study are as listed in the tables (3-2), (3-3), (3-4) and (3-5) :

Table 3- 2: Elastic property of the concrete material

compressive strength	Young modulus	Poisson ratio
35 MPa	27805 Mpa	0.2

Table 3- 3: Plastic property of the concrete material

Dilation angle	Eccentricity	Fb_0/fc_0	K	Viscosity parameter
30	0.1	1.16	0.667	0.0011

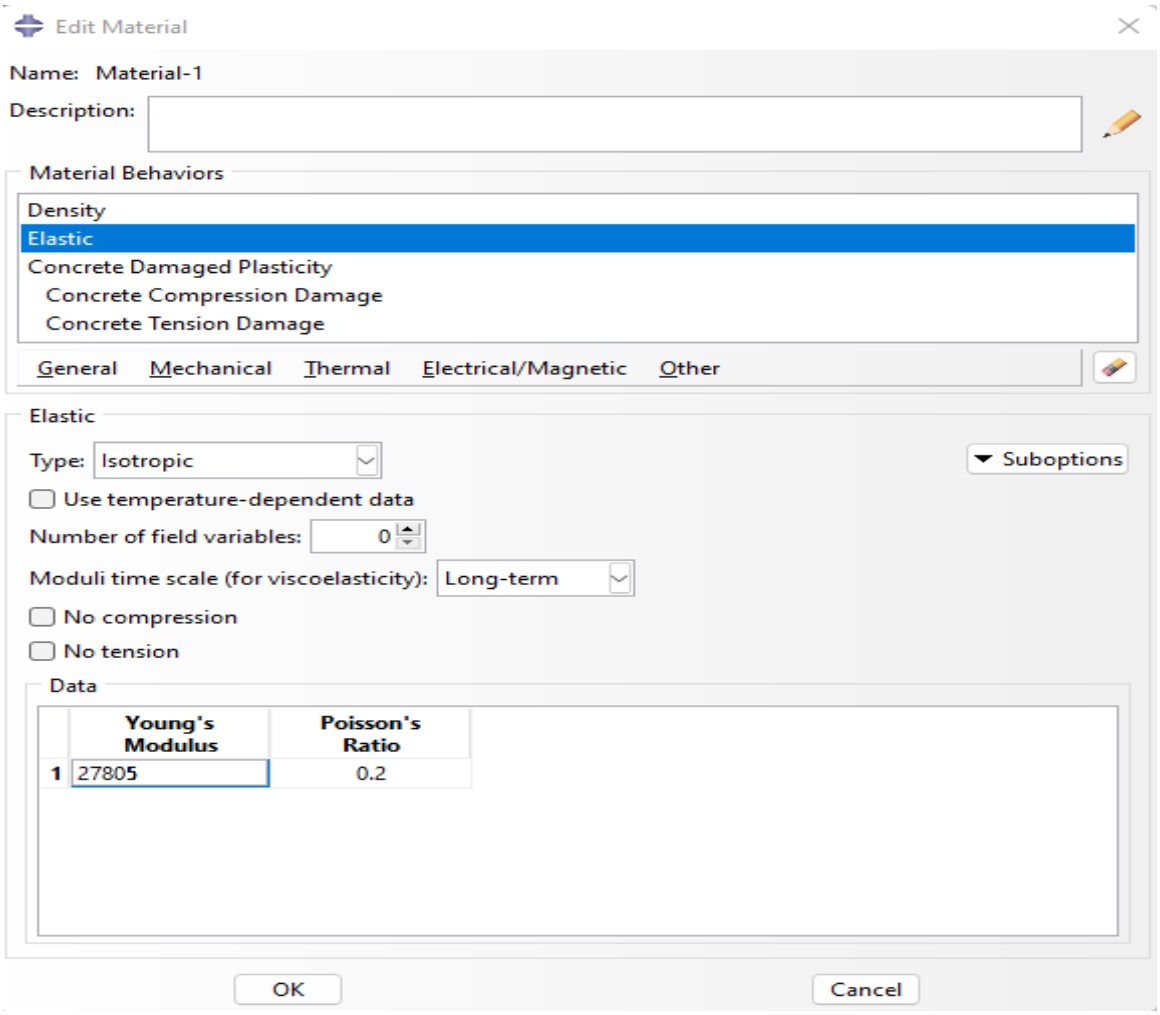

Plate 3-12: Defining elastic property of the concrete material

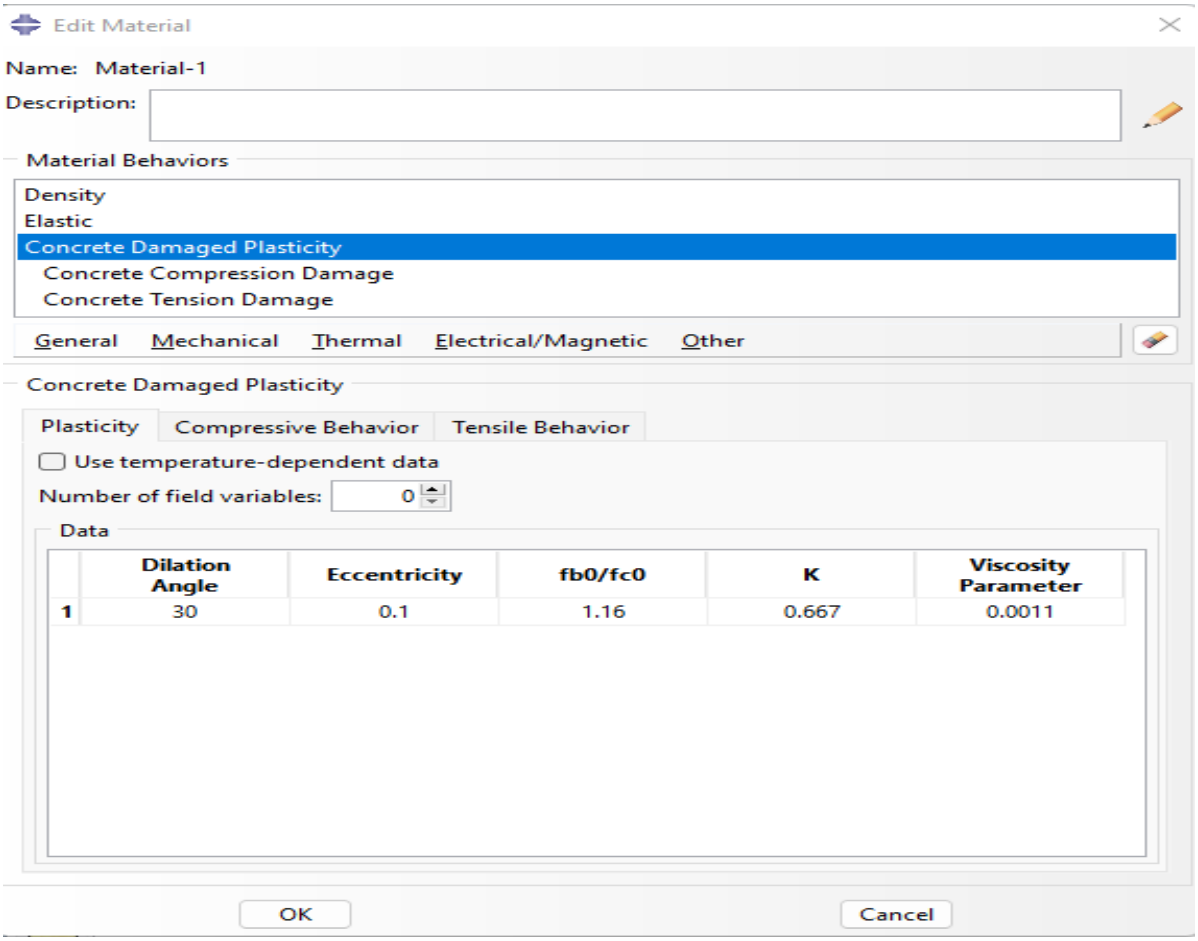

Plate 3-13: Defining plastic property of the concrete material

Table 3- 4: Relationship of the Stress-Strain of concrete (Tensile behaviour).

Yield stress	Cracking strain
3.857979	0
3.007118	0.000125516
2.58214	0.000238261
2.313008	0.000346332
2.121924	0.000452062
1.976701	0.000556417
1.686502	0.00086512
1.505766	0.00117054
1.378614	0.001474353
1.282538	0.001777234
1.206441	0.002079516
1.144117	0.002381385
1.061184	0.002883873
0.996084	0.003385825
0.943113	0.003887413
0.898851	0.004388741
0.8611	0.004889873
0.810699	0.005691384
0.769313	0.006492625
0.734489	0.00729367
0.704624	0.008094565
0.672623	0.009095525
0.645192	0.010096348
0.621316	0.011097064
0.535535	0.016099636
0.480668	0.021101282
0.441496	0.026102456
0.411619	0.031103352

Table 3- 5: Relationship of the Stress-Strain of concrete (compressive behaviour).

Yield stress	Inelastic strain
20.26479	0
25.46725	2.34381E-05
29.8845	6.99147E-05
33.51109	0.000139777
36.34152	0.000233186
38.37023	0.000350306
39.59161	0.000491302
40	0.000656341
39.86246	0.00084559
39.4491	0.00105922
38.75879	0.001194186
37.7904	0.001337423
36.54279	0.001488966
35.01483	0.001648848
33.20535	0.001817103
31.11321	0.001993766
28.73724	0.002178871
26.07628	0.002372453
23.12915	0.002574547
19.89466	0.002785187
16.37164	0.003004409
12.55888	0.003232248
8.455185	0.003468741
4.059348	0.003713922
	0.003967828
	0.004230495

3.4.4 Meshing and convergence studies

The concrete model regarding hollow-core slab system are modelled by using an eight-node brick element (C3D8) as can be observed in Plate 3-14.

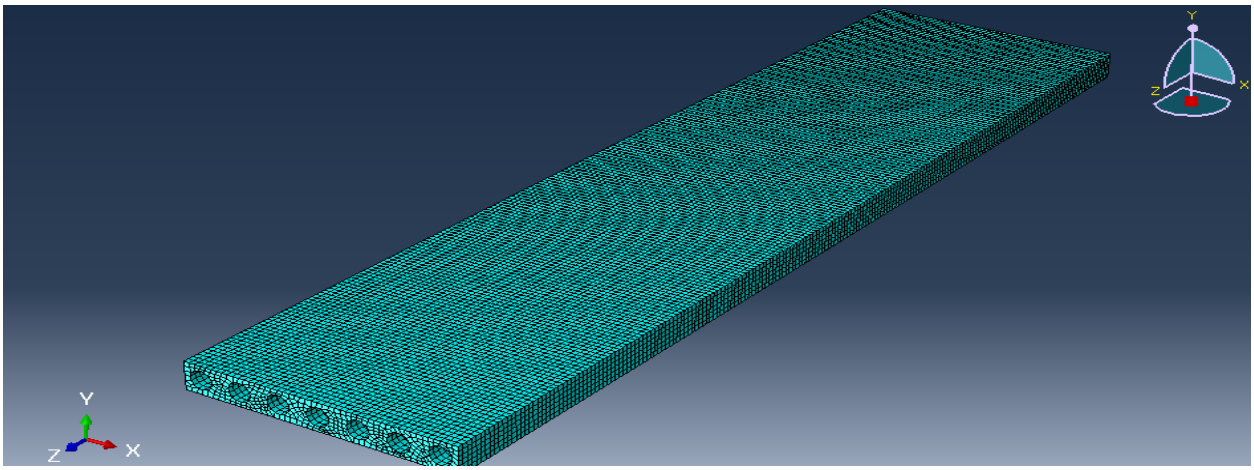

Plate 3-14: Mesh of model

The proper mesh size with the minimum number of elements and maximum convergence can be done by the convergence study. Practically can be achieved by running analysis several times with same material property and minimizing (twenty-five numbers) of the meshing size for each running attempt starting from (150mm) up to (25mm) of the mesh size. The recorded results obtained by the analysis running attempts clarify that the differences of displacements can be ignored when the mesh size decreased from (75 mm) to (25mm). Therefore, the (50mm) is adopted for all models analysed using **ABAQUS Standard/Explicit 2020.**

3.4.5 Loading and boundary conditions

The boundary conditions regarding the supports in this research study is simply supported case which is modelled as a single line of nodes. To simulate the roller support case, all of the aforesaid nodes are free to move in the direction of y-

axis only while constrained the displacements for the rest of axes in addition to constrained the rotation in all axis as clearly observed in the Plate 3-15.

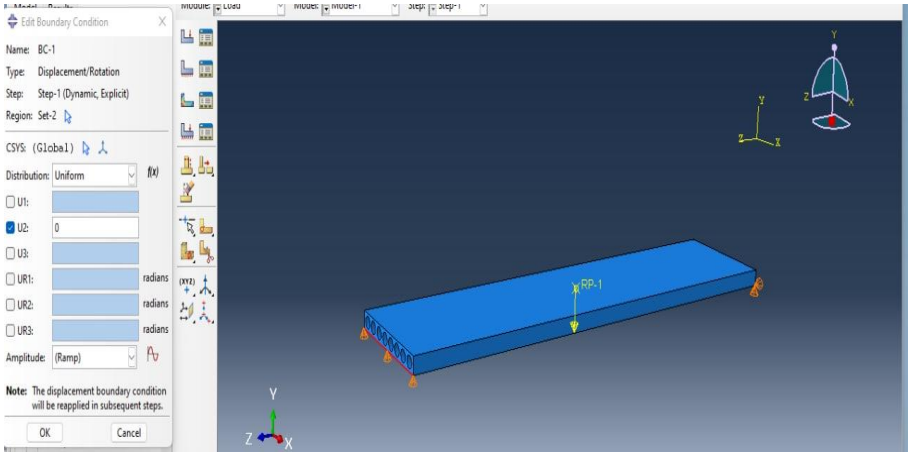

Plate 3-15: Roller support as one of boundary condition.

In case of the modelling the hinge support, the single line of nodes is constrained for the movement in the direction of z- axis, free to move in the directions of x-axis and y-axis. Moreover, rotational movements are constrained for all axes as clearly shown in the Plate 3-16.

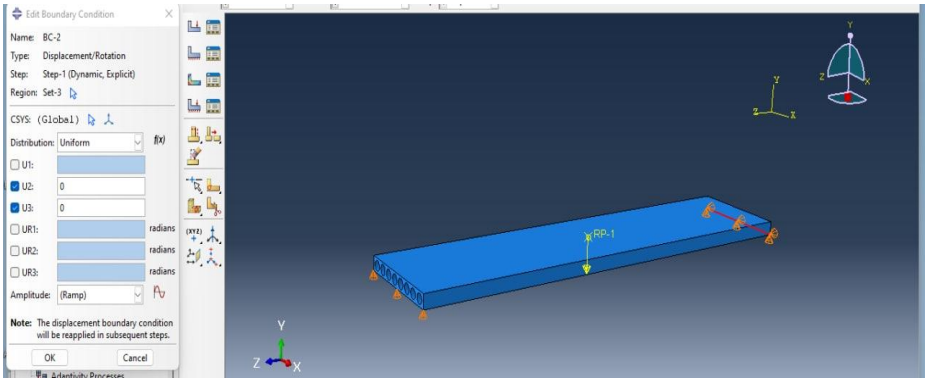

Plate 3-16: Hinge support of boundary condition.

And input load by amplitude as shown in plate 3-17.

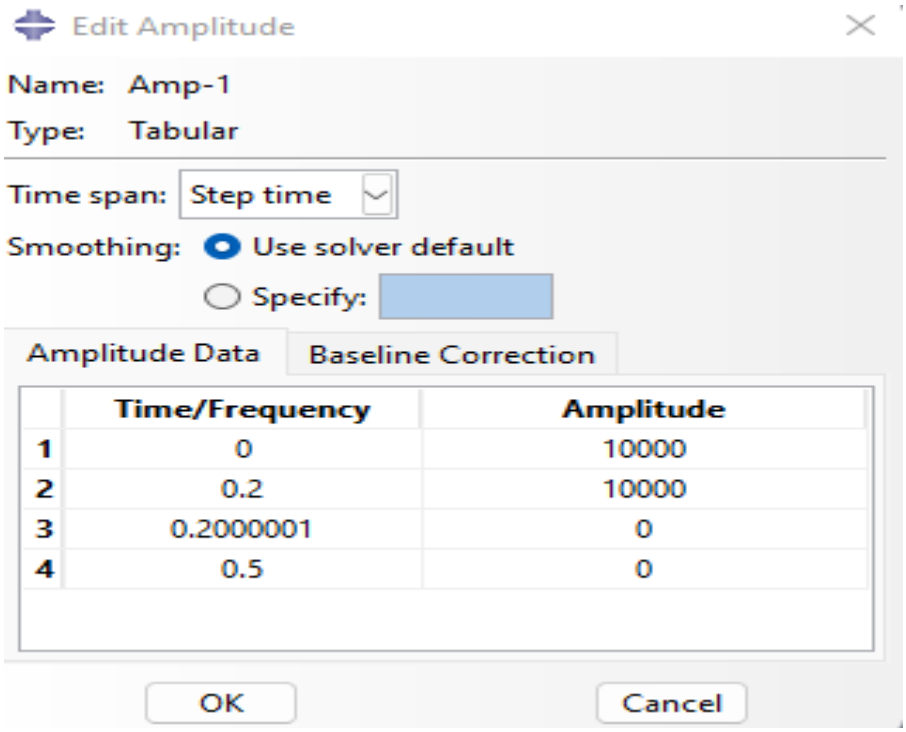

Plate 3-17: Amplitude load.

3.4.6 Desirable results from analysis

In order to investigate the dynamic performance of the hollow-core slab units, the change of the displacements with time are studied by the results of finite element analysis as clearly observed in the Plate 3-18.

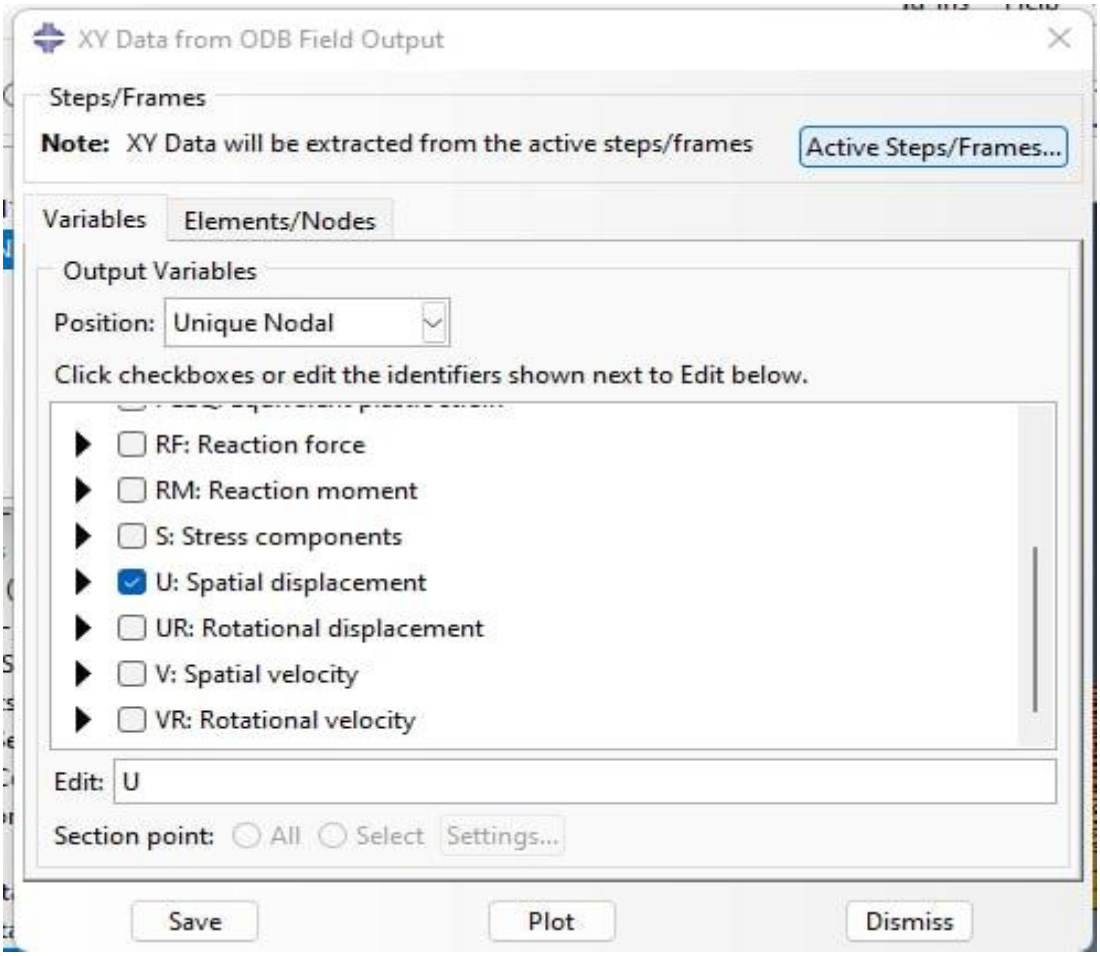

Plate 3-18: Change of displacement with time.

the results obtained by ABAQUS Standard/Explicit 2020 are compared with the Visual Basic programing language outcomes for two model only which is representing two case of the loading conditions (rectangular pulse load and triangular pulse load) that discussed in previous sections. Visual Basic results already induced and obtained based on the model analytical studies.

3.5 Summary

This chapter of analytically various states of material which are supposed to be the material model of the hollow-core slab. The elastic state of the material model gives a general awareness of its structural behaviour and also gives an

introduction of its performance in the next stage which is the elastoplastic state. In the case of the elastoplastic stage of the material model, the analytical solutions have clarified the importance of studying this stage regarding its virtual results. Moreover, in order to solve as well as examine more complicated cases of the applied load for the two-state of material models separately, the **Visual Basic** programming language has been utilized. The outcomes obtained by **Visual Basic** well match the analytical solutions, which will be furthermore discussed in chapter four. In one case, regarding the applied load affecting hollow-core slab that modelled by **ABAQUS Standard/Explicit 2020**, which is well simulated its shape configuration, the load applications, and its boundary conditions, the dynamic performance regarding the change of displacement with time has been investigated too.

Chapter Five
Conclusions and Recommendations

5.1 Conclusions

In this chapter, the conclusions based on the results of analytical studies, **Visual Basic** programming language, and Finite-Elements-Analysis by using **ABAQUS** Standard/Explicit 2020, are presented. The analytical study of the hollow slab model was carried out for two different material models as mentioned in previous chapters which are elastic and elastoplastic material models. Hollow-core slab as the structural element under various cases of the impact loads has been analysed analytically and by using programs as well. The effect of geometric configuration shape of the slab voids, as well as the effect of various sizes of these voids, has been studied. The load-carrying capacity of the hollow-core slab elements is evaluated based on the effect of the aforesaid variables on the displacements-time-history and vibration frequency as well.
From the results of analysis, the following conclusions can be made as follows:

1. **Influence of the slab voids**:

- Changing the geometric configuration shape of the voids from circular to square shape within a similar equivalent cross-sectional area has no obvious effect on both the displacement-time-history and the vibration frequency for all cases of the applied load.
- Changing the size of the voids for the two cases of voids which are circular and square in shape has noticeable effect on both the

displacement-time-history and the vibration frequency for all cases of the applied load. In particular, the displacements increase as the size of the openings of the slab void increase. This could be related to the fact of the stiffness as well as inertia moment of the hollow-core slab units decreased as the size of the opening increased.

2. Influence of the material model:

- The material models clarified previously, are elastic range and elastoplastic range. In both cases, these material models exhibit linear relations for the applied impact load and the displacement-time history. The reasons that explained such behaviours of the material models need additional in-quasi-static studies to describe in detail the material model response.

3. Influence of the different types of pulse-load:

- Response of the hollow-core slab units that were subjected to different types of the pulse load, and based on the results obtained regarding **Max.** Displacement can be concluded that the **Rectangular** -pulse load is the worst case compared to **Triangular** the -pulse load. Therefore, in order to have comprehensive understanding that explain the reasons are need for further experimental studies.

5.2 Recommendations

- Among the factors affecting the load carrying capacity of the hollow-core slab units, whether square or circle the opening size of the slab voids either require further attention. Studying effect of the opening size of the slab voids while, subjected to harmonic loading conditions is a

great of deal. Moreover, studying the effect of using larger size of voids with fill in material which putting inside the inner space of voids, for instance, polystyrene foam as an acceptable economic choice which might be a revolutionary option in the production field of precast concrete elements.

- Regarding to the fact of using such types of slabs in warehouse containing working machines therefore, studying the effect of harmonic loading cases is a great of deal.
- Since the Visual Basic programming language indicate an acceptable outcome, therefore carrying out the approximate method is interesting topic to be researched.

References

[1] D. K. B. Renee A Lindsay, John B Mander, “Experiments on the seismic performance of hollow-core floor systems in precast concrete buildings,” Proceedings of the 13th World Conference on Earthquake Engineering, Vancouver, no. 585, pp. 1–15, 2004.

[2] “Prestressed hollow-core slabs on load bearing masonry,” 2009.

[3] W. Hollowcore, “DESIGN DATA.”

[4] P. P. C. Committee, Manual for Quality Control for Structural Precast Concrete Products. 1999.

[5] P. Hollowcore and F. Solutions, “THE CORE OF THE High quality ,.”

[6] NPCAA, “Hollow Core Flooring - Technical Manual,” 2003.

[7] Nordimpianti, “Hollow Core Slabs Applications,” 2017.

[8] ASSAP, The Hollow Core Floor Design and Applictions. 2002.

[9] “hollow-core.pdf.”

[10] U. As and V. Walling, “Prestressed hollowcore concrete slabs.”

[11] T. Precast and C. Slab, HOLLOW-CORE CONCRETE SLABS. .

[12] I. R. For, P. Concrete, and H. Core, “Inspection of Production Items on the Construction Site Unloading , Hoisting Interim Storage,” 2008.

[13] F. Liu, “Dynamic analysis of hollow core concrete floors,” p. 64, 2018.

[14] EnCon Design, “Hollow-core Building System Design Manual,” 2015, pp. 1–38.

[15] M. Paz and S. Halperson, Structural Dynamics: Theory and Computation, vol. 102, no. 3. 1980.

[16] S. Assist and A. Almadany, “NATURAL VIBRATION FREQUENCIES AND MODES FOR UNDAMPED SYSTEM :,” pp. 1–22.

[17] A. K. Chopra, Dynamics of Structures—Theory and Applications to Earthquake Engineering, Third Edition, vol. 23, no. 2. 2007.

[18] F. Liu, J. M. Battini, C. Pacoste, and A. Granberg, “Experimental and Numerical Dynamic Analyses of Hollow Core Concrete Floors,” Structures, vol. 12, no. September, pp. 286–297, 2017.

[19] A. Maazoun, J. Vantomme, and S. Matthys, “Damage assessment of hollow core reinforced and prestressed concrete slabs subjected to blast loading,” Procedia Engineering, vol. 199, pp. 2476–2481, 2017.

[20] A. Maazoun, S. Matthys, B. Belkassem, D. Lecompte, and J. Vantomme, “Blast response of retrofitted reinforced concrete hollow core slabs under a close distance explosion,” Engineering Structures, vol. 191, no. October 2018, pp. 447–459, 2019.

[21] F. Liu, J. M. Battini, and C. Pacoste, “Finite element modelling for the dynamic analysis of hollow-core concrete floors in buildings,” Journal of Building Engineering, vol. 32, no. May, p. 101750, 2020.

[22] K. A. Chebo, Y. Temsah, Z. A. Saleh, M. Darwich, and Z. Hamdan, “Experimental Investigation on the Structural Performance of Single Span Hollow Core Slab under Successive Impact Loading,” Materials, vol. 15, no. 2, 2022.

[23] L. K. Marcos and R. Carrazedo, “Parametric study on the vibration sensitivity of hollow-core slabs floors,” Proceedings of the International Conference on Structural Dynamic , EURODYN, vol. 2014-Janua, no. July, pp. 1095–1102, 2014.

[24] M. I. Rahimi, A. G. N. H, M. J. Z, and Z. Ibrahim, “Ambient Vibration Response of Precast Hollow Core Flooring System,” no. February, 2020.

[25] J. M. BIGGS, Introduction-to-Structural-Dynamics-Biggs.pdf. .

[26] Weiler company" Hollow core slabs" German company, www.weiler .net